Journal of Cleaner Production 572 (2026) 148924

Contents lists available at ScienceDirect

Journal of Cleaner Production

journal homepage: www.elsevier.com/locate/jclepro

Life cycle and economic assessment of inverted p-i-n perovskite solar cells

Joana Príncipe [a], Luísa Andrade [a,*], Vera C.M. Duarte [a], Teresa M. Mata [b], António A. Martins [c,**]

[a] LEPABE - Laboratory for Process Engineering, Environment, Biotechnology and Energy, ALiCE - Associate Laboratory in Chemical Engineering, Faculty of Engineering, University of Porto, Rua Dr. Roberto Frias, Porto, 4200-465, Portugal
[b] LAETA - Associated Laboratory for Energy, Transports and Aerospace, INEGI - Institute of Science and Innovation in Mechanical and Industrial Engineering, Rua Dr. Roberto Frias 400, Porto, 4200-465, Portugal
[c] CBQF - Center for Biotechnology and Fine Chemistry - Associated Laboratory, School of Biotechnology, Portuguese Catholic University, Rua Diogo Botelho 1327, Porto, 4169-005, Portugal

HIGHLIGHTS

- Cradle-to-grave LCA of an inverted perovskite solar cell is performed.
- The life cycle global warming emissions are 0.20 kg CO_2 eq./kWh.
- The energy payback time is calculated to 0.53 years.
- This work also analyses the energy payback time for a regular perovskite solar cell.

GRAPHICAL ABSTRACT

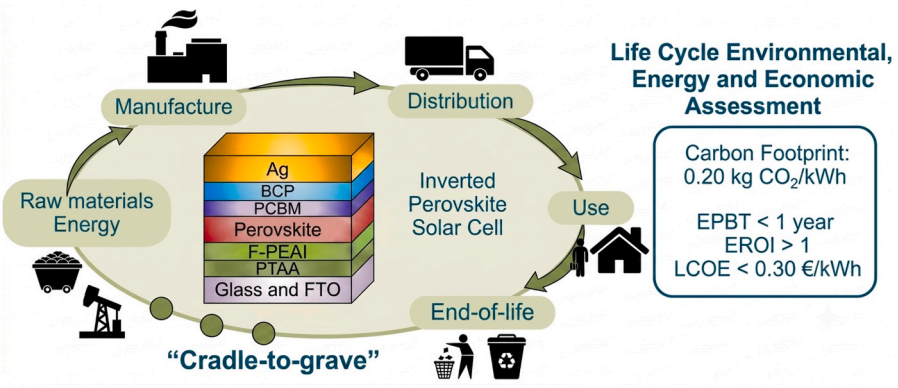

ARTICLE INFO

Keywords:
Inverted perovskite solar cells
Cradle-to-grave analysis
Life cycle assessment (LCA)
Cumulative energy demand (CED)
Energy payback time (EPBT)
Levelized cost of electricity (LCOE)

ABSTRACT

Photovoltaic technologies hold significant potential for meeting the world's growing energy demands. Among emerging alternatives to conventional silicon-based solar cells, perovskite solar cells (PSCs) have attracted increasing attention for their promising efficiency and cost-effectiveness. This study aims to evaluate the sustainability performance of an inverted PSC, addressing a critical gap in the integrated assessment of this emerging technology. A cradle-to-grave life cycle assessment (LCA) was conducted, combined with energetic and economic analyses, evaluating energy payback time (EPBT), energy return on investment (EROI), and levelized cost of electricity (LCOE). A sensitivity analysis was performed to assess the influence of key operational parameters. The results show a carbon footprint of 0.20 kg CO_2 eq./kWh and a cumulative energy demand of 4.88 MJ/kWh. The system exhibits an EPBT of 0.53 years and an EROI of 9.50, while the LCOE is estimated at 0.29 €/kWh, for a PSC production cost at 0.67 €/cm^2. The sensitivity analysis indicates that the PCE and degradation rates are the main drivers of energetic performance, whereas the LCOE remains relatively stable. Additionally,

* Corresponding author.
** Corresponding author.
E-mail addresses: landrade@fe.up.pt (L. Andrade), aaamartins@ucp.pt (A.A. Martins).

https://doi.org/10.1016/j.jclepro.2026.148924
Received 10 February 2026; Received in revised form 27 May 2026; Accepted 5 July 2026
Available online 9 July 2026

EPBT and EROI are strongly influenced by solar irradiance and local climatic conditions. These findings highlight that, despite the relatively low manufacturing impacts, improvements in PCE, operational lifetime, and degradation rates are essential for enhancing the overall sustainability and economic viability of PSCs. The main contribution of this work lies in providing a multidimensional (environmental, energetic, and economic) baseline assessment of inverted PSCs, offering novel insights into the key parameters that will determine their future commercial competitiveness.

1. Introduction

In 2024, global electricity consumption increased by nearly 1100 TWh (Rolf Frischknecht et al., 2020), and it is projected to continue growing in the coming years, primarily driven by rapid electrification of end-use sectors, in particular in buildings and transportation (Ember, 2024). This demand is expected to rise at an average annual rate of 3.4 % through 2026 (International Energy Agency, 2024). As population growth and rising living standards improve energy needs increase, and a continued reliance on fossil fuels will further increase greenhouse gas emissions and exacerbate climate change negative impacts.

In this context, the Paris Agreement establishes the objective of limiting the global average temperature increase to below 2 °C above pre-industrial levels, while pursuing efforts to restrict it to 1.5 °C (United Nations Framework Convention on Climate Change, 2015). Achieving these targets requires a rapid transition towards renewable energy systems. In the European Union (EU), this transition has been supported by policy frameworks such as the Renewable Energy Directive (2009/28/EC) (European Parliament and Council of the European Union, 2009), which defined policies and goals to increase the share of renewables in the EU from 12.5 % in 2010 to 25.4 % in 2024 (European Environment Agency, 2025). The revised directive (2018/2001/EU) (European Parliament and Council of the European Union, 2018), effective from December 2018 as part of the Paris Agreement commitments, set a new binding target of at least 32 % renewable energy by 2030. In light of the ongoing economic and energy crisis, a provisional agreement reached in March 2023 sets a binding target of at least 42.5 % by 2030, with an ambition of reaching 45 % (European Commission, 2023).

Among renewable energy sources, solar energy is widely recognized as a key option, due to its abundance and broad geographical availability. Moreover, photovoltaic (PV) technologies have become increasingly cost-competitive, exhibiting lower levelized costs of electricity compared to fossil-based generation (U.S. Energy Information Administration, 2025; Lazard. Lazard, 2025). Global installed PV capacity has expanded significantly in recent years, from 0.023 TW in 2009 (Statistical, 2023) to 2.2 TW in 2024 (International Energy Agency, 2025). However, solar energy still accounted for only approximately 10 % of global electricity consumption in 2024 (International Energy Agency, 2025), highlighting the need for further improvements in efficiency, cost, and scalability of existing and/or future PV technologies.

Currently, first-generation PV technologies, mainly based on crystalline silicon, dominate the market, with a market share exceeding 90 % (Osman and Qureshi, 2025). Despite their maturity and reliability, these technologies involve energy-intensive manufacturing processes and the use of hazardous chemicals, which can limit their sustainability and application potential. Second-generation PV technologies have emerged, including thin-film PVs such as amorphous silicon, cadmium telluride, and copper indium gallium diselenide, offering improved light absorption and reduced material usage. These technologies can exhibit absorption coefficients 10 to100 times higher than crystalline silicon, owing to their advanced active layer properties. However, these advantages do not yet translate into competitive electricity generation costs, which remain higher when compared to the dominant silicon based technologies (Príncipe et al., 2022). Third-generation PV technologies, such as dye-sensitized, quantum dot, organic, polymer, and inorganic-organic perovskite solar cells (PSCs), have emerged as promising alternatives, offering the potential for higher efficiency, low production costs, scalability, and reduced environmental impacts (Wang et al., 2016). Among these, PSCs have attracted particular attention due to their rapid technological evolution, and in this article, a specific type of PSC is analysed.

PSCs typically consist of a perovskite light-absorbing layer sandwiched between electron and hole transport layers (ETL and HTL), together with charge-collecting electrodes (Said et al., 2019). Upon light absorption, the perovskite film generates electrons and holes, which are transferred to the ETL and HTL, respectively, before being collected by the electrodes (Liu et al., 2016). PSCs exist in two main configurations: regular n-i-p, in which the perovskite layer is deposited on the ETL followed by the HTL; and the inverted p-i-n, where the sequence is reversed. Inverted PSCs are currently attracting more interest due to their simpler fabrication, reduced operational hysteresis, and lower sintering temperature (Said et al., 2019; Xu et al., 2019; Jiang et al., 2019). These cells have achieved a power conversion efficiencies (PCEs) of up to 27.3 %, approaching the 27.9 % record of crystalline silicon solar cells (NREL, 2026). Considering that the first inverted PSC, reported in 2013, exhibited a modest PCE of 3.9 % (Jeng et al., 2013), this rapid progress highlights their remarkable technological potential. Despite these advances, PSCs still remain at an early stage of development (technology readiness level ~4), corresponding to laboratory-scale proof of concept. Key challenges, particularly related to long-term stability and environmental performance, continue to hinder their large-scale commercialization. In this context, LCA and the economic evaluation of the PV technologies are essential methodologies for evaluating the environmental impacts and the economic variability of PSCs across their entire life cycle, from raw material extraction to end-of-life, identifying which factors control they potential and need to be tackled in R&D activities to ensure they are a viable option to currently dominant technologies (ISO 14040, 2006; ISO 14044, 2006).

As PSCs gain prominence as a promising PV technology, the number of LCA and/or economic studies has grown substantially in recent years (Espinosa et al., 2015; Gong et al., 2015; Celik et al., 2016; Alberola-Borràs et al., 2018a, 2018b, 2018c; Maranghi et al., 2019; Sarialtin et al., 2020; Chakraborty et al., 2021; Guerrero et al., 2021; Rao et al., 2021; Rodriguez-Garcia et al., 2021; Tian et al., 2021; Li et al., 2022a; Okoroafor et al., 2022; McCalmont et al., 2023; Weyand et al., 2023; Purkayastha et al., 2024; Ravilla et al., 2024; Chaosukho et al., 2024; Zhao et al., 2024; Rossi et al., 2024; Kamali et al., 2024; Leccisi and Fthenakis, 2024; Lee et al., 2025; Príncipe et al., 2025; Clegg et al., 2025; Valderrama et al., 2025; Larini et al., 2025; Herrera et al., 2025; Ma et al., 2025; Kralj et al., 2025; Luu et al., 2026; Jech et al., 2026). However, these studies vary widely in scope, system boundaries and underlying assumptions. Some focus solely on manufacturing impacts (cradle-to-gate), while others extend to the operational phase, incorporating assumptions regarding lifetime, PCE, and degradation rates. A subset of studies also considers the end-of-life stage, addressing disposal or material recovery (cradle-to-grave or cradle-to-cradle approaches, respectively). Differences in system boundary definitions and methodological assumptions further contribute to the variability of reported results, making it harder to compare different studies and to adequately define lines of R&D. To address this, section 2 presents a review of all studies that specifically examine inverted PSCs. To the best of our knowledge, apart from our previous work (Príncipe et al., 2025),

no study has assessed the PSC structure analysed in this work, which is among the most efficient configurations reported to date (Liu et al., 2020; Degani et al., 2021; Li et al., 2022b; Jiang et al., 2022). This highlights a significant gap in the literature, as most previous research has not provided a comprehensive evaluation of such advanced configurations.

This present study fills that gap by conducting a cradle-to-grave LCA and economic evaluation of an inverted PSC with the structure glass/FTO/PTAA/F-PEAI/$Cs_x[(CH_3(NH_2)_2)_{1-y}(CH_3NH_3)_y]_{1-x}Pb(I_{1-z}Br_z)_3$/PCBM/BCP/Ag. The primary objective is to assess the environmental, energetic, and economic performance of this novel PSC configuration, providing critical insights into its potential for large-scale deployment.

To validate the energetic advantages of the inverted architecture, a targeted comparison of energy payback time (EPBT) was performed against a regular PSC architecture with the structure: glass/FTO/c-TiO_2/m-TiO_2/$Cs_x[(CH_3(NH_2)_2)_{1-y}(CH_3NH_3)_y]_{1-x}Pb(I_{1-z}Br_z)_3$/spiro-OMeTAD/Au. A subsequent sensitivity analysis evaluated the influence of PCE, operational lifetime, and degradation rate on global warming value, EPBT, energy return on investment (EROI) and levelized cost of electricity (LCOE) values. Additionally, given the strong influence of solar irradiance and climate on PV performance, multiple European locations with diverse climates were considered. The study also examined the effects of replacing the Portuguese electrical mix with those of France, Germany, Greece, or Poland, as well as the implications of transitioning to a fully renewable electricity mix in these countries.

This manuscript is organized as follows. Section 2 presents a critical review of the literature on LCA of PSCs, highlighting gaps related to inverted architectures. Section 3 describes the methodological framework, including the assumptions and models used for the environmental, energy, and economic assessments. Section 4 reports and discusses the main results, including the baseline scenario and sensitivity analyses. Finally, Section 5 summarizes the key findings and discusses their implications for the future development and large-scale implementation of PSC technologies.

2. Literature review

A growing body of literature evaluates the environmental impacts of PSC production using the LCA methodology (Espinosa et al., 2015; Gong et al., 2015; Celik et al., 2016; Alberola-Borràs et al., 2018a, 2018b, 2018c; Maranghi et al., 2019; Sarialtin et al., 2020; Chakraborty et al., 2021; Guerrero et al., 2021; Rao et al., 2021; Rodriguez-Garcia et al., 2021; Tian et al., 2021; Li et al., 2022a; Okoroafor et al., 2022; McCalmont et al., 2023; Weyand et al., 2023; Purkayastha et al., 2024; Ravilla et al., 2024; Chaosukho et al., 2024; Zhao et al., 2024; Rossi et al., 2024; Kamali et al., 2024; Leccisi and Fthenakis, 2024; Lee et al., 2025; Príncipe et al., 2025; Clegg et al., 2025; Valderrama et al., 2025; Larini et al., 2025; Herrera et al., 2025; Ma et al., 2025; Kralj et al., 2025; Luu et al., 2026; Jech et al., 2026) (Table 1). Despite the growing interest in PSC technologies, the literature studies specifically addressing inverted PSC architectures remain scarce. To contextualize the present work, this section provides a critical review of existing LCA studies of PSCs, focusing on inverted PSCs.

Espinosa et al. (2015) apply LCA to evaluate an inverted spin-coated PSC with the structure glass/ITO/PEDOT:PSS/$CH_3NH_3PbI_{3-x}Cl_x$/PCBM/Al. For this PSC, non-renewable energy use decreases from 59.55 MJ in the first year to 53.98 MJ after 15 years, indicating reduced energy demand over its lifespan. Climate change impact drops from 5.24 kg CO_2 eq. in the first year to 0.35 kg CO_2 eq. after 15 years, reflecting the long-term efficiency of the PSC. Human health impact, measured in potential years of life lost, decreases from 2.27×10^{-8} to 1.50×10^{-8} CTUh/pers, and freshwater ecotoxicity falls from 85.02 to 5.67 CTUe/pers over 15 years. The energy payback time improves significantly, reducing from 16.54 to 1.10 years. Overall, despite higher initial impacts, long-term use leads to substantial reductions, making this PSC a promising option for sustainable energy production.

Guerrero et al. (2021) conducted a cradle-to-gate LCA of inverted PSC with the structure glass/ITO/PEDOT:PSS/$CH_3NH_3PbI_3$/PCBM/Au. The study found that perovskite PVs have low energy requirements, with the typical regular configuration (glass/FTO/c-TiO_2/m-TiO_2/$CH_3NH_3PbI_3$/spiro-OMeTAD/Au) consuming 255.76 kWh/m^2, while the inverted configuration uses 154.25 kWh/m^2 (0.015 kWh/cm^2). Modifying heat treatment and deposition processes can further reduce energy consumption for the inverted configuration. Additionally, the fluorine-doped tin oxide (FTO) substrate contributes the most to the embedded energy, emphasizing the need for FTO recycling to minimize environmental impact.

Rodriguez-Garcia et al. (2021) conducted an LCA study examining the recycling of coated glass substrates in both regular and inverted PSCs. Their research compared the environmental impacts of 13 PSC recycling techniques, focusing on chemical, thermal, and physical delamination processes for recovering coated glass. The study revealed that material consumption was the primary driver of ecotoxicity, which significantly contributed to the overall environmental impact. Notably, the analysis revealed that all but one of the recycling techniques resulted in higher environmental impacts compared to the production of virgin coated glass. This underscores the need for further optimization of recycling methods to minimize their ecological footprint.

Li et al. (2022a) studied the environmental impact of producing a perovskite solar module with the structure PET/graphene/P3HT/$CH_3NH_3PbI_3$+AVAI/PCBM/Ag, obtaining 9.55 ± 1.05 kg CO_2 eq./m^2 for a 2-year lifespan and estimating 4 g CO_2 eq./kWh for a 25-year lifespan.

Okoroafor et al. (2022) highlights the environmental advantages of inkjet printing for PSCs compared to spin-coating method. A cradle-to-gate LCA showed significant improvements in all impact categories for inkjet-printed PSCs. Specifically, the global warming potential (GWP) was measured at 7.54 kg CO_2 eq./m^2 and the cumulative energy demand at 200.18 MJ/m^2 for a PSC with the structure PET/I-ZO/PEDOT:PSS/$Cs_{0.1}[(CH(NH_2)_2)_{0.83}(CH_3NH_3)_{0.17}]_{0.9}Pb(I_{0.83}Br_{0.17})_3$/$C_{60}$/BCP/Ag operating over 20 years. These values were significantly lower than the ones obtained via spin-coating method, that exhibited a GWP of 74.5 kg CO_2 eq./m^2 and cumulative energy demand of 1204 MJ/m^2. The authors also found that a green solvent-based precursor ink resulted in up to six orders of magnitude lower environmental impacts than conventional toxic solvents, offering opportunities for improving PSC sustainability.

Purkayastha et al. (2024) estimated a total primary energy demand of 643.98 MJ/m^2 for the development of tin-based perovskite solar modules with the structure glass/ITO/PEDOT:PSS/$CH_3(NH_2)_2SnI_3$/PCBM/Ag. The authors observed that the ITO glass contributes to nearly 37.09 % of the total primary energy demand and is the major bottleneck for reducing the energy consumption. Moreover, the group obtained a carbon footprint of 0.07 kg CO_2 eq./kWh.

Ravilla et al. (2024) obtained a GWP of 0.00498 kg CO_2 eq./kWh for a PSC using black phosphorus quantum dots (BPQDs) as low-dimensional material to enhance the hole extraction of PEDOT:PSS on a device with the structure glass/FTO/PEDOT:PSS + BPQDs/$CH_3NH_3PbI_3$/PCBM/Ag.

In our previous study (Príncipe et al., 2025), a cradle-to-gate LCA analysis was conducted to compare the production of regular and inverted PSCs, using the following structures: glass/FTO/c-TiO_2/m-TiO_2/$Cs_x[(CH_3(NH_2)_2)_{1-y}(CH_3NH_3)_y]_{1-x}Pb(I_{1-z}Br_z)_3$/spiro-OMeTAD/Au for the regular PSC, and glass/FTO/PTAA/F-PEAI/$Cs_x[(CH_3(NH_2)_2)_{1-y}(CH_3NH_3)_y]_{1-x}Pb(I_{1-z}Br_z)_3$/PCBM/BCP/Ag for the inverted PSC. The results showed that the production of the regular PSC has a higher environmental impact than the inverted PSC, primarily due to differences in material and energy consumption. Specifically, regular PSCs require about 132 MJ/cm^2 compared to 25 MJ/cm^2 for the inverted PSC, leading to carbon footprints of 14.1 kg CO_2 eq./cm^2 and 2.31 kg CO_2 eq./cm^2, respectively. Moreover, for the inverted PSC, energy consumption accounts for about 80 % of the total environmental impact. In contrast, for the regular PSC, the dominant contributor varies by impact category, with both materials and energy playing significant roles.

Table 1
– Overview of LCA studies on PSCs published to date, including PSC architecture and structure, LCA approach, functional unit, and reported environmental impact metrics when available.

Ref.	Year	Architecture	PSC Structure	LCA Approach	FU[a]	GWP[b]
Espinosa et al. (2015)	2015	Regular and Inverted	Glass/FTO/c-TiO_2/$CH_3NH_3PbI_{3-x}Cl_x$/spiro-OMeTAD/Ag Glass/ITO/PEDOT:PSS/$CH_3NH_3PbI_{3-x}Cl_x$/PCBM/Al	Cradle-to-gate	Energy produced (kWh)	5.48 → 0.37 kg CO_2 eq./kWh (1 – 15 years) 5.24 → 0.35 kg CO_2 eq./kWh (1 – 15 years)
Gong et al. (2015)	2015	Regular	Glass/FTO/c-TiO_2/m-TiO_2/$CH_3NH_3PbI_3$/spiro-OMeTAD/Au Glass/ITO/ZnO/$CH_3NH_3PbI_3$/spiro-OMeTAD/Ag	Cradle-to-grave	Area (m^2)	21.7 g CO_2 eq./m^2 19.1 g CO_2 eq./m^2
Celik et al. (2016)	2016	Regular	Glass/FTO/SnO_2/$CH_3NH_3PbI_3$/CuSCN/MoO_x/Al Glass/FTO/SnO_2/$CH_3NH_3PbI_3$/C-paste	Cradle-to-gate	Energy produced (kWh)	99 – 147 g CO_2 eq./kWh
Alberola-Borràs et al. (2018a)	2018	Regular	Glass/FTO/c-TiO_2/m-TiO_2/$CH_3NH_3PbI_3$+AVAI/spiro-OMeTAD/Au Glass/FTO/c-TiO_2/m-TiO_2/$CH_3NH_3PbI_3$+AVAI/ZrO_2/C	Cradle-to-gate	Energy produced (kWh)	9.50 kg CO_2 eq./kWh 0.165 kg CO_2 eq./kWh
Alberola-Borràs et al. (2018b)	2018	Regular	Glass/FTO/c-TiO_2/$CH_3NH_3PbI_3$/spiro-OMeTAD/Au Glass/FTO/c-TiO_2/m-TiO_2/$CH_3NH_3PbI_3$/spiro-OMeTAD/Au	Cradle-to-grave	Area (cm^2)	0.000517 kg CO_2 eq./cm^2 0.00951 kg CO_2 eq./cm^2
Alberola-Borràs et al. (2018c)	2018	-	Focuses only on the perovskite layer	Cradle-to-gate	Area (cm^2)	n.r.
Maranghi et al. (2019)	2019	Regular	Glass/FTO/TiO_2/$CH_3NH_3PbI_3$/spiro-OMeTAD/Au Glass/ITO/ZnO/$CH_3NH_3PbI_3$/spiro-OMeTAD/Ag Glass/FTO/TiO_2/$CH_3NH_3PbI_3$/spiro-OMeTAD/Ag Glass/FTO/TiO_2/$CH_3NH_3SnI_3$/spiro-OMeTAD/Au Glass/FTO/TiO_2 nanotube/$CH_3NH_3PbI_3$/Iodine/Pt glass Glass/FTO/SnO_2/$CH_3NH_3PbI_3$/CuSCN/MoO_x-Al (solution-based deposition) Glass/FTO/SnO_2/$CH_3NH_3PbI_3$/CuSCN/MoO_x-Al (vacuum-based deposition) Glass/FTO/SnO_2/$CH_3NH_3PbI_3$/C-Paste	Cradle-to-gate	Area (m^2)	n.r.
Sarialtin et al. (2020)	2020	Regular	Glass/FTO/c-TiO_2/m-TiO_2/$CH_3NH_3PbI_3$/C-paste Glass/FTO/SnO_2/$CH_3NH_3PbI_3$/C-paste	Cradle-to-gate	Area (m^2), Energy produced (kWh)	75 g CO_2 eq./kWh 94 g CO_2 eq./kWh
Chakraborty et al. (2021)	2021	Regular	Glass/FTO/TiO_2/Cs_2TiBr_6/CuSCN/Ag Glass/FTO/TiO_2/Cs_2TiI_6/CuSCN/Ag Glass/FTO/TiO_2/Cs_2TiCl_6/CuSCN/Ag Glass/FTO/TiO_2/Cs_2TiF_6/CuSCN/Ag Glass/FTO/TiO2/$Cs_2TiI_{6-x}Br_x$/CuSCN/Ag	Cradle-to-grave	Energy produced (kWh)	n.r.
Guerrero et al. (2021)	2021	Regular and Inverted	Glass/FTO/c-TiO_2/m-TiO_2/$CH_3NH_3PbI_3$/spiro-OMeTAD/Au Glass/ITO/PEDOT:PSS/$CH_3NH_3PbI_3$/PCBM/Au	Cradle-to-gate	Area (m^2)	n.r.
Rao et al. (2021)	2021	Regular	Glass/FTO/TiO_2/$Cs_x[(CH_3(NH_2)_2)_{1-y}(CH_3NH_3)_y]_{1-x}Pb(I_{1-z}Br_z)_3$/spiro-OMeTAD/Au	Cradle-to-grave	Energy produced (kWh)	182 g CO_2 eq./kWh
Rodriguez-Garcia et al. (2021)	2021	Regular and Inverted	Glass/ITO/PEDOT:PSS/$CH_3NH_3PbI_3$/PCBM/CA/Al Glass/ITO/NiO_x/$CH_3NH_3PbI_3$/PCBM/BCP/Ag Glass/FTO/TiO_2/$CH_3NH_3PbI_3$/Au:NiO_x Glass/FTO/TiO_2/$CH_3NH_3PbI_3$/C Glass/FTO/TiO_2/$CH_3NH_3PbI_3$/spiro-OMeTAD/Ag Glass/FTO/TiO_2/$CH_3NH_3PbI_3$/spiro-OMeTAD/Au Glass/FTO/TiO_2/$CH_3(NH_2)_2Li_{0.85}$+$CH_3NH_3LBr_{0.15}$/spiro-OMeTAD/Au Focuses only on the recycling of the coated glass substrate	-	Area (m^2)	n.r.
Tian et al. (2021)	2021	Regular	Glass/FTO/c-TiO_2/LBSO/$CH_3NH_3PbI_3$/PTAA/Cu	Cradle-to-cradle	Energy produced (kWh)	13.4 g CO_2 eq./kWh
Li et al. (2022a)	2022	Inverted	PET/graphene/P3HT/$CH_3NH_3PbI_3$+AVAI/PCBM/Ag	Cradle-to-gate	Area (m^2)	9.55 ± 1.05 kg CO_2 eq./m^2 (2-year lifespan) 4 g CO_2 eq./kWh (25-year lifespan)
Okoroafor et al. (2022)	2022	Inverted	PET/IZO/PEDOT:PSS/$Cs_{0.1}[(CH(NH_2)_2)_{0.83}(CH_3NH_3)_{0.17}]_{0.9}Pb(I_{0.83}Br_{0.17})_3$/$C_{60}$/BCP/Ag	Cradle-to-gate	Energy produced (kWh)	7.54 kg CO_2 eq./m^2
McCalmont et al. (2023)	2023	-	Focuses on the recovery of the perovskite materials	-	Area (m^2)	n.r.
Weyand et al. (2023)	2023	Regular	Glass/FTO/c-TiO_2/m-TiO_2/$CH_3NH_3PbI_3$/spiro-OMeTAD/Au	Cradle-to-gate	Energy produced (kWh), Area (m^2)	25 – 500 kg CO_2 eq./m^2
Purkayastha et al. (2024)	2024	Inverted	Glass/ITO/PEDOT:PSS/$CH_3(NH_2)_2SnI_3$/PCBM/Ag	Cradle-to-grave	Area (m^2)	0.07 kg CO_2 eq./kWh

(*continued on next page*)

Table 1 (*continued*)

Ref.	Year	Architecture	PSC Structure	LCA Approach	FU[a]	GWP[b]
Ravilla et al. (2024)	2024	Regular and Inverted	Glass/FTO/SnO_2+graphene/$CH_3NH_3PbI_3$+BP/spiro-OMeTAD + rGO/Ag Glass/FTO/SnO_2+GQDs/$CH_3NH_3PbI_3$+rGO/spiro-OMeTAD + BP/Ag Glass/FTO/SnO_2+graphene/$CH_3NH_3PbI_3$+BP/CuSCN + rGO/Ag Glass/FTO/PEDOT:PSS + BPQDs/$CH_3NH_3PbI_3$/PCBM/Ag	Cradle-to-grave	Energy produced (kWh)	4.55 g CO_2 eq./kWh 7.46 g CO_2 eq./kWh 4.56 g CO_2 eq./kWh 4.98 g CO_2 eq./kWh
Chaosukho et al. (2024)	2024	Regular	Glass/FTO/SnO_2/$Cs_x[(CH_3(NH_2)_2)_{1-y}(CH_3NH_3)_y]_{1-x}PbI_3$/spiro-OMeTAD/Au Glass/FTO/SnO_2/$Cs_x[(CH_3(NH_2)_2)_{1-y}(CH_3NH_3)_y]_{1-x}PbI_3$/spiro-OMeTAD/C-paste	Cradle-to-gate	Energy produced (kWh)	2.32 kg CO_2 eq./kWh 0.33 kg CO_2 eq./kWh
Zhao et al. (2024)	2024	Regular	Glass/ITO/SnO_2/$Cs_x[(CH_3(NH_2)_2)_{1-y}(CH_3NH_3)_y]_{1-x}Pb(I_{1-z}Br_z)_3$/spiro-OMeTAD/Au PET/ITO/SnO_2/$Cs_x[(CH_3(NH_2)_2)_{1-y}(CH_3NH_3)_y]_{1-x}Pb(I_{1-z}Br_z)_3$/spiro-OMeTAD/Au PET/ITO/SnO_2/$Cs_x[(CH_3(NH_2)_2)_{1-y}(CH_3NH_3)_y]_{1-x}Pb(I_{1-z}Br_z)_3$/spiro-OMeTAD/C	Cradle-to-grave	Area (m^2)	570.3 kg CO_2 eq./m^2 105 kg CO_2 eq./m^2 3.0 kg CO_2 eq./m^2
Rossi et al. (2024)	2024	Regular	Glass/FTO/c-TiO_2/m-TiO_2/$Cs_x[(CH_3(NH_2)_2)_{1-y}(CH_3NH_3)_y]_{1-x}Pb(I_{1-z}Br_z)_3$/spiro-OMeTAD/Au Glass/FTO/c-TiO_2/C_{60}/$(CH_3(NH_2)_2)_{1-y}(CH_3NH_3)_yPbI_3$/spiro-OMeTAD/Au	Cradle-to-gate	Area (cm^2)	n.r.
Kamali et al. (2024)	2024	Regular	Glass/ITO/SnO_2/$K_{0.025}(Cs_{0.1}FA_{0.9})_{0.975}PbI_3$/spiro-OMeTAD/Au	Cradle-to-grave	Mass (kg)	2.83 – 6.20 kg CO_2 eq./kg
Leccisi and Fthenakis (2024)	2024	Regular	Glass/FTO/SnO_2/$CH_3NH_3PbI_3$/CuSCN/MoO_x/Al Glass/ITO/SnO_2/$CH_3NH_3PbI_3$/CuSCN/MoO_x/Al Glass/FTO/PCBM/$CH_3NH_3PbI_3$/NiO_x/Ag	Cradle-to-gate	Area (m^2)	n.r.
Lee et al. (2025)	2025	-	Evaluates the environmental impacts of several lead recycling processes in PSCs	-	-	n.r.
Príncipe et al. (2025)	2025	Regular and Inverted	Glass/FTO/c-TiO_2/m-TiO_2/$Cs_x[(CH_3(NH_2)_2)_{1-y}(CH_3NH_3)_y]_{1-x}Pb(I_{1-z}Br_z)_3$/spiro-OMeTAD/Au Glass/FTO/PTAA/F-PEAI/$Cs_x[(CH_3(NH_2)_2)_{1-y}(CH_3NH_3)_y]_{1-x}Pb(I_{1-z}Br_z)_3$/PCBM/BCP/Ag	Cradle-to-gate	Area (cm^2)	14.1 kg CO_2 eq./cm^2 2.31 kg CO_2 eq./cm^2
Clegg et al. (2025)	2025	-	Compares the environmental impacts of lead-based with lead-free halide perovskite absorber layers and derivates	Cradle-to-grave	Area (cm^2)	n.r.
Valderrama et al. (2025)	2025	Inverted	Glass/ITO/NiO_x/Al_2O_3/$CH_3NH_3PbI_3$/PCBM/Ag	Cradle-to-gate	Area (cm^2), Energy produced (kWh)	0.015 kg CO_2 eq./cm^2
Larini et al. (2025)	2025	Regular	Glass/ITO/SnO_2/$FAPbI_3$/spiro-OMeTAD/Au	Cradle-to-grave/ Cradle-to-cradle	Area (cm^2)	n.r.
Herrera et al. (2025)	2025	-	Evaluates the environmental impacts of different recycling methods for PSCs	-	Area (m^2)	n.r.
Ma et al. (2025)	2025	-	Comparative life cycle toxicity impact assessment of lead-based and lead-free PSCs	Cradle-to-grave	Energy produced (kWh)	n.r.
Kralj et al. (2025)	2025	-	Glass/ITO/SAMs/$Cs_{0.15}FA_{0.85}Pb_{2.76}Br_{0.24}$/$MgF_2$/$C_{60}$/BCP/Ag Focuses on the recycling of the coated glass substrate	Cradle-to-grave	Area (m^2)	9 – 13 kg CO_2 eq./cm^2
Luu et al. (2026)	2026	Regular	Glass/ITO/MgF_2/SnO_2/$CH_3NH_3PbI_3$/a-Si:H/Au Glass/ITO/MgF_2/SnO_2:Ru/$CH_3NH_3PbI_3$/MoO_3/Au Glass/ITO/MgF_2/SnO_2/$Cs_x[(CH_3(NH_2)_2)_{1-y}(CH_3NH_3)_y]_{1-x}Pb(I_{1-z}Br_z)_3$/$MoO_3$/Au Glass/FTO/$TiO_2$/$CH_3NH_3PbI_3$/spiro-OMeTAD/Au	Cradle-to-grave	Energy produced (kWh)	0.58 – 6.18 kg CO_2 eq./kWh
Jech et al. (2026)	2026	Regular	Glass/FTO/c-TiO_2/m-TiO_2/m-ZrO_2/$CH_3NH_3PbI_3$ infiltrated/C Glass/FTO/c-TiO_2/m-TiO_2/m-Al_2O_3/$CH_3NH_3PbI_3$ infiltrated/NiO Glass/FTO/c-TiO_2/m-TiO_2/m-Al_2O_3/$CH_3NH_3PbI_3$ infiltrated/Au:NiO Focuses on the recycling approach	Cradle-to-end of second-life	Energy produced (kWh)	n.r.

[a] FU = Functional Unit, which can be area (m^2 or cm^2) or energy produced (kWh), depending on the study.

[b] GWP = Global Warming Potential, expressed in kg CO_2 equivalent per functional unit, as reported in the original studies. For studies reporting ranges over device lifetime, the first value corresponds to the initial year and the second to the final year (where applicable). Values have been included only when explicitly reported in the original publications; other environmental impact categories are discussed in the text. "n.r." = not reported in the referenced study.

Valderrama Benítez et al. (Valderrama et al., 2025) conducted a cradle-to-grave LCA of a PSC with the structure glass/-ITO/NiO_x/Al_2O_3/$CH_3NH_3PbI_3$/PCBM/Ag. The study compared this inverted PSC to commercial solar cells and found that it exhibited lower environmental impacts, primarily due to reduced energy demands and the use of fewer hazardous materials. The authors also observed that the lead content in the perovskite layer contributed insignificantly to key environmental categories, including human carcinogenic toxicity and ecotoxicity in water. Additionally, the energy analysis revealed that manufacturing energy consumption varies by location, suggesting that PSCs could be competitive with commercial solar technologies in terms of greenhouse gas emissions, provided their operational lifetime exceeds 10 years.

3. Methods

The environmental impact of the lab-scale PSC was evaluated through a life cycle perspective, considering the entire life cycle of the inverted PSC architecture. This assessment encompasses raw material extraction and processing, energy consumption, device fabrication, usage, and end-of-life treatment, including material recycling and final disposal.

3.1. Life cycle assessment

This study evaluates the environmental impacts associated with the production, use and disposal of an inverted PSC using the LCA methodology, in accordance with the International Organization for Standardization (ISO) 14040[22] and 14044 (ISO 14044, 2006) standards. The LCA is conducted in four stages: 1) Goal and scope definition: this stage defines the goal, objectives, system components and processes, boundaries, and the functional unit; 2) Inventory analysis: all inputs and outputs are compiled for the system; 3) Impact assessment: the environmental impacts of the system are evaluated based on the inventory data collected in stage 2; and 4) Interpretation: the results are analysed and discussed to derive conclusions (ISO 14040, 2006; ISO 14044, 2006; Burnley et al., 2019). The following sections outline the key aspects and assumptions used in the development of this study.

3.1.1. Goal definition

This study aims to conduct a cradle-to-grave LCA of an inverted PSC prepared in a laboratory at the Faculty of Engineering of the University of Porto (FEUP), Portugal. The LCA covers the entire life cycle, from manufacturing (cradle) through the use phase to the disposal phase (grave). Since the PSCs are prepared at a laboratory scale, it was possible to directly measure the materials and energy consumptions during the manufacturing of the solar cells. It should be noted that these measured values represent upper-limit consumptions, rather than the levels expected under industrial conditions. Nevertheless, the authors believe that the conclusions from this study remain valid, at least qualitatively, for future upscaling and industrial implementation.

3.1.2. Scope definition

Functional Unit: The chosen functional unit (FU) is 1 kWh of energy produced by the PSCs, and all generated inventories were converted to this functional unit. The FU aligns with the primary function of the PSC, which is to generate electricity, typically measured in kWh (Ardente et al., 2025; Frischknecht et al., 2020).

System Boundary: The system boundary, illustrated in Fig. 1, encompasses the three main stages of the life cycle assessment: production, operation, and end-of-life of the PSC. The production stage includes the extraction of raw materials and all subsequent processes up to the production of the PSC. After the PSC has been used, some materials are recycled, while the remaining components are considered waste to be disposed of. Transportation of raw materials is also included, with materials assumed to be transported from European suppliers to the production site by truck, or by ship and truck if the supplier is located outside Europe, specifically in Australia. Emissions related to transportation from the production site to the point of use and from there to the point of disposal are also considered. This study used an attributive life cycle assessment approach, where environmental impacts are assigned to the defined FU. Hence, it will be easier to compare the results with different architectures or solar cells based on other technologies. The analysis does not account for system-wide changes resulting from displacing conventional grid electricity with energy generated by the PSC under study, as it is still under development and far from wide commercial application. No allocation procedures between life cycle inventory items and co-products were required for the manufacturing phase, as the system produces a single product and the production facilities are dedicated exclusively to its fabrication. For the end-of-life stage, a standard cut-off approach was applied. Under this approach, the environmental impacts associated with the dismantling and recycling processes are included within the system boundaries, while no environmental credits are claimed for the subsequent use of the recovered materials. Whenever possible, Portuguese and European conditions were considered in the assessment, particularly regarding the energy and electricity consumed during the recycling process.

Materials Used in PSC Production: The PSC was produced at laboratory scale using materials sourced from various suppliers. FTO-coated glass substrates (7 $\Omega \cdot sq^{-1}$) were obtained from Greatcell Solar Materials. Bathocuproine (BCP) was purchased from Sigma-Aldrich. Poly[bis(4-phenyl)(2,4,6-trimethylphenyl)amine (PTAA) and (European Environment Agency, 2025European Environment Agency, 2025)-phenyl-C61-butyric acid methyl ester (PCBM) were supplied from Ossila. The 4-fluoro-phenethylammonium iodide compound (F-PEAI) compound was sourced from TCI Europe N.V. Perovskite films were fabricated using lead iodide (PbI_2), and lead bromide ($PbBr_2$) from TCI Europe N.V., cesium iodide (CsI) from Sigma-Aldrich, and formamidinium iodide (FAI) and methylammonium bromide (MABr) from Greatcell Solar Materials. Anhydrous solvents [2-propanol, chlorobenzene, dimethyl sulfoxide (DMSO), *N*,*N*-dimethylformamide (DMF) and toluene] were purchased from Sigma-Aldrich. Acetone and 2-propanol were acquired from VWR, and silver (Ag) pellets were sourced from Kurt J. Lesker.

PSC Production: The first stage of the life cycle involves the extraction of the raw materials required to produce all components and solutions for manufacturing the inverted PSC. This stage encompasses all processes, from mineral extraction to the transformation of these

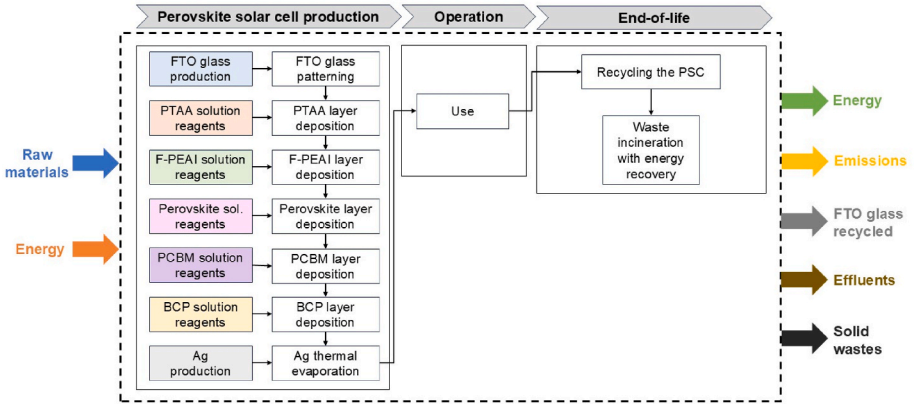

Fig. 1. – Cradle-to-grave system boundary of the PSC LCA, including production, operation, and end-of-life stages. No direct emissions are assumed during operation. FTO glass recycling is modelled using a cut-off approach, with no credits assigned to recovered materials.

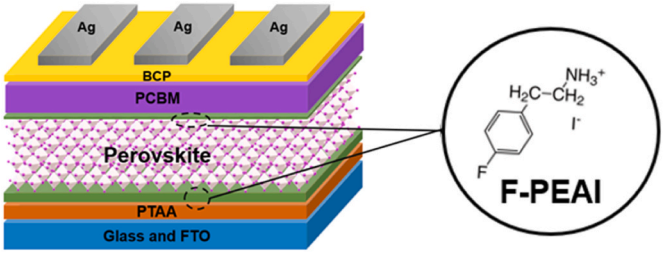

Fig. 2. – Structure of the PSC used in this study.

minerals into useable materials. The PSC has a layered structure, with the deposition of each layer occurring sequentially from bottom to top, as shown in Fig. 2.

The procedure for preparing the inverted PSC follows a method reported elsewhere (Degani et al., 2021), and enables the production of batches comprising 20 cells simultaneously. First, FTO glass substrates were washed with a 10 % aqueous Hellmanex solution. The substrates were then cleaned sequentially through ultrasonic treatment with deionised water for 5 min, followed by acetone and 2-propanol for 10 min in each solvent. After cleaning, the substrates were dried with a nitrogen flow and treated with oxygen plasma at 100 mW for 10 min before depositing the active layers. All depositions, except for the back-contact layer, were performed using a spin-coater inside of a glovebox filled with an inert nitrogen atmosphere.

First, 50 µL of a PTAA solution (1.5 mg/mL in toluene) were spin-coated at 2000 rpm for 40 s and then annealed at 100 °C for 10 min. After annealing, the samples were washed with 100 µL of an F-PEAI solution in DMF (5 mg/mL) by spin-coating at 4000 rpm for 30 s. Next, the perovskite film was deposited. A perovskite precursor solution of 1.2 M $Cs_{0.05}(FA_{0.85}MA_{0.15})_{0.95}Pb(I_{0.85}Br_{0.15})_3$ was prepared by mixing different cations (Pb, Cs, FA, and MA) and halides (I and Br) in a solvent mixture of DMF/DMSO (4:1), using a 10 % excess of PbI_2. The perovskite layer was fabricated by depositing 60 µL of the precursor solution using a two-step spin-coating procedure: first at 1000 rpm for 12 s, followed by 5000 rpm for 27 s. At 21 s into the second spin-coating step, 100 µL of antisolvent (a 0.125 mg/mL solution of F-PEAI in a chlorobenzene/2-propanol mixture, 9:1) were dripped onto the spinning substrate. Subsequently, the samples were annealed at 100 °C for 30 min. After annealing, the substrates were allowed to cool, and then 50 µL of a 20 mg/mL PCBM solution in chlorobenzene were spin-coated onto the perovskite layer at 2000 rpm for 30 s (with a ramping speed of 1000 rpm/s). The PCBM films were then annealed at 100 °C for 10 min. Next, 50 µL of a 0.5 mg/mL BCP solution in 2-propanol were spin-coated at 4000 rpm for 30 s (with a ramping speed of 1000 rpm/s) to form a buffer layer. Finally, 80 nm of Ag were thermally evaporated onto the substrates to complete the process.

PSC Operation: The initial PCE was assumed to be 18.8 %, corresponding to the maximum PCE achieved by the lab-scale PSC under study in the host laboratory (Principe et al., 2025). During operation, the PSCs themselves do not generate waste or emissions, as they produce electricity directly from solar energy. However, the maintenance of PSC devices (*e.g.*, soil cleaning, balance of the system (BOS) replacement, repairing panel breakdowns, and addressing leakage) over their lifetime requires energy and results in emissions. The lifetime of PSCs remains under investigation. A common benchmark in the PV industry is the T_{80} lifetime, defined as the time over which a device retains 80 % of its initial PCE (He et al., 2020). Comparative studies report average annual degradation rates for different PV technologies: crystalline silicon-based devices at ~ 0.5 %, amorphous silicon 0.87 %, cadmium telluride 0.4 %, copper indium gallium selenide 0.96 %, monocrystalline silicon 0.36 %, and polycrystalline silicon 0.64 % (Jordan and Kurtz, 2013). Based on the T_{80} lifetime threshold, achieving a 10-year lifetime for perovskite-based technologies would require a maximum degradation rate of 2 % per year. However, the lifetime of the PSCs can be limited by both intrinsic factors (*e.g.,* thermal stability and light soaking stability of the perovskite materials) and external factors (*e.g.,* moisture, oxygen, and metal electrode migration) (He et al., 2020). As a result, a baseline scenario assuming a 5-year lifetime with a constant degradation rate of 4 % per year was considered. Given this relatively short lifetime, the environmental impacts associated with the maintenance stage are assumed to be negligible, as soil cleaning has relatively low environmental impacts compared to the other stages of the system (Rao et al., 2021). Additionally, BOS replacement and panel breakdown are considered unlikely. And even if panel breakdown and leakage occur, several mitigation methods, such as physical encapsulation and chemical absorption, have been reported to minimize their effects (Wu et al., 2022). Therefore, the environmental impacts during the operation phase were considered negligible.

PSC End-of-life Scenario: The end-of-life stage includes the environmental impacts related to separating the various layers of a PV device, recycling certain components, and disposing others. Two common end-of-life scenarios typically considered for solar cells are landfill disposal or incineration with energy recovery. For this study, it was assumed that the FTO-coated glass substrate would be recycled, while the remaining components of the PSC would undergo incineration with energy recovery and flue gas treatment targeting heavy metals and halides. The dismantling and recycling of the FTO-coated glass substrates were modelled based on a study by Príncipe et al. (Principe et al., 2023), which demonstrated that FTO-coated glass can be recycled and reused multiple times with minimal impact on its properties and the efficiency of PSCs. In the recycling process for the FTO-coated glass from the assembled PSCs, the Ag electrode was removed using Scoth® tape. The remaining layers were then removed ultrasonically using a 1.5 M potassium hydroxide solution in 70 % ethanol for 5 min. Afterward, the glass substrates were cleaned in an ultrasonic bath with distilled water for 5 min, dried using a nitrogen flow, and prepared for reuse (Principe et al., 2023).

3.1.3. *Life cycle inventory analysis*

The life cycle inventory (LCI) for this study is based on primary data collected from the lab-scale production of PSCs, which covers the foreground processes. This data is complemented with literature sources for the background processes, including the production of raw materials for PSC manufacturing, their transportation to the production site, and the generation of the consumed energy, accounting for the distance between the supplier and the laboratory. All energy consumption is assumed to be electricity sourced from the Portuguese low-voltage grid.

A list of the materials used in PSC production, along with details on how the LCI data were obtained, is provided in Table 2. For most materials, the LCI data were sourced from the ecoinvent database v3.9.1, available in the SimaPro™ v9.5.0.1 software (PhD version), or from relevant scientific and technical literature. Necessary calculations were made to adjust the data to the functional unit selected for this study.

Table 2 shows that LCI data for F-PEAI, PTAA and Scotch® tape were unavailable, requiring modelling of their life cycles to estimate their environmental impacts.

While the most rigorous approach would involve using specialized software, such as Aspen Plus Process Simulation Tool, to model the production of these compounds, this was not feasible due to the lack of key kinetic and thermodynamic data. Instead, an alternative strategy based on the tree-like structure of LCA was adopted, focusing on the upstream processes needed to produce each compound. When LCI data for a compound are not available, it is possible to estimate the inventory by tracing the production flows back to points where reliable data exist. Basic information such as reaction stoichiometry, molar masses, and precursor materials is used, typically sourced from chemistry textbooks, encyclopaedias, patents, and scientific literature (Geisler et al., 2004; Huber et al., 2022). This approach has been used successfully in various studies, including for ionic liquids (Zhang et al., 2008; Cuéllar-Franca et al., 2016) and for estimating the carbon footprint of PSCs (Carneiro

Table 2
– Materials used in PSC production and end-of-life stage, and corresponding inventory data sources.

Material	LCI data source	Dataset
2-propanol	ecoinvent v3.9.1	Isopropanol {RER} | market for isopropanol | Cut-off, S
F-PEAI	Not found	-
PCBM	Ref. (Tsang et al., 2016)	Table S1 of Supplementary data
Ethanol	ecoinvent v3.9.1	Ethanol, without water, in 99.7 % solution state, from fermentation {Europe without Switzerland} | dewatering of ethanol from biomass, from 95 % to 99.7 % solution state | Cut-off, S
Acetone	ecoinvent v3.9.1	Acetone, liquid {RER} | market for acetone, liquid | Cut-off, S
BCP	Ref. (Celik et al., 2017)	Table S2 of Supplementary data
CsI	Ref. (Khalifa et al., 2020)	Table S3 of Supplementary data
Chlorobenzene	ecoinvent v3.9.1	Monochlorobenzene {RER} | market for monochlorobenzene | Cut-off, S
Deionised water	ecoinvent v3.9.1	Water, deionised {Europe without Switzerland} | market for water, deionised | Cut-off, S
DMSO	ecoinvent v3.9.1	Dimethyl sulfoxide {GLO} | market for dimethyl sulfoxide | Cut-off, S
FTO substrate	Ref. (Gong et al., 2015)	Table S4 of Supplementary data
FAI	Ref. (Alberola-Borràs et al., 2018c)	Table S5 of Supplementary data
$PbBr_2$	Ref. (Alberola-Borràs et al., 2018c)	Table S6 of Supplementary data
PbI_2	Ref. (Alberola-Borràs et al., 2018c)	Table S7 of Supplementary data
MABr	Ref. (Alberola-Borràs et al., 2018c)	Table S8 of Supplementary data
DMF	ecoinvent v3.9.1	N,N-dimethylformamide {GLO} | market for N,N-dimethylformamide | Cut-off, S
PTAA	Not found	-
Ag	ecoinvent v3.9.1	Silver {GLO} | market for silver | Cut-off, S
Toluene	ecoinvent v3.9.1	Toluene, liquid {RER} | market for toluene, liquid | Cut-off, S
Scotch® tape	Not found	-
Potassium hydroxide	ecoinvent v3.9.1	Potassium hydroxide {GLO} | market for potassium hydroxide | Cut-off, S

et al., 2022).

In this study, different strategies were applied depending on the compound. F-PEAI was modelled using stoichiometric calculations based on its precursors (phenethylamine, benzyl cyanide), with detailed calculations of masses per functional unit. Scotch® tape was modelled based on its main constituents (cellulose acetate, acrylic mixture, and adhesive), using background inventory data from ecoinvent v3.9.1 for each component. A detailed description of the modelling strategies and the resulting inventory data for F-PEAI and Scotch® tape are provided in the Supplementary data (section 2). For PTAA, the complexity of its synthesis prevented this approach, so a generic organic chemical dataset from ecoinvent v3.9.1 was adopted (Chemical, organic {GLO} \| chemical production, organic \| Cut-off, S).

To calculate the LCI data per FU, it is necessary to estimate the electricity generated during the operational lifetime of the PSC (E_{gen}). This requires accounting for the operational stability of the PSC. In this study, an annual degradation rate of 4 % was applied. The PCE degradation was modelled as a compound annual reduction, where the PCE in any given year of operation, *t*, is calculated by reducing the previous year's efficiency, as expressed in equation (1):

$$PCE_t = PCE_{initial} \times (1-d)^{t-1} \quad (1)$$

where $PCE_{initial}$ (%) is the initial power conversion efficiency assumed, d (%) is the degradation rate of the PSC, and t is the year of operation over the PSC's lifetime.

Accordingly, the annual energy generation, E_t (kWh) for a specific year t is calculated using the degraded PCE value for that year:

$$E_t = I \times A \times PCE_t \times PR \quad (2)$$

where I (kWh/m^2 year) is the annual solar irradiation, A (m^2) is the active area of the PSC, and PR (%) is the performance ratio of the PV technology, accounting for system losses. The annual solar irradiation varies depending on the geographic location. In this study, the PSC was fabricated in a laboratory at FEUP, Portugal (coordinates: 41° 10′ 40.8″ N, 8° 35′ 49.2″ W). To estimate I, the Photovoltaic Geographical Information System (PVGIS) webtool (Huld et al., 2012) was utilized. PVGIS provides open-access data on solar radiation and temperature for global PV performance assessments. It calculates the optimal tilt angle for solar devices at specific locations to maximize irradiance and estimates the average annual irradiation based on monthly irradiation values. In this study, I was estimated as 1897.32 kWh/m^2 year. The active area of the PSC is 1 cm^2, representing 35 % of the total FTO glass substrate area. The PR is assumed to be 75 % (Celik et al., 2018; Frischknecht et al., 2016; Yue et al., 2014).

The total lifetime electricity generation (E_{gen}) is thus calculated as the sum of the annual energy outputs over the entire assumed lifetime (LT) of the PSC:

$$E_{gen} = \sum_{t=1}^{LT} E_t \quad (3)$$

This approach provides a robust estimation of the PSC's lifetime electricity generation, accounting for key factors such as location-specific solar irradiance and overall system performance.

3.1.4. Environmental impact assessment

To the best of the authors' knowledge, no established product category rules or standardized guidelines currently exist for conducting environmental assessments of solar cells, regardless of the technology family. Consequently, selecting an appropriate life cycle impact assessment methodology requires considering both its relevance to the specific product system under investigation and its prevalence in existing LCA literature to ensure comparability.

In this study, the ReCiPe 2016 midpoint method (egalitarian

Table 3
– Potential environmental impact categories calculated using the RECIPE 2016 method.

Environmental impact category	Acronym	Unit
Global Warming	GW	kg CO_2 eq.
Stratospheric Ozone Depletion	SOD	kg CFC-11 eq.
Ionizing Radiation	IR	kBq Co-60 eq.
Ozone Formation Human Health	OFHH	kg NO_x eq.
Fine Particulate Matter Formation	FPMF	kg $PM_{2.5}$ eq.
Ozone Formation Terrestrial Ecosystems	OFTE	kg NO_x eq.
Terrestrial Acidification	TA	kg SO_2 eq.
Freshwater Eutrophication	FETP	kg P eq.
Marine Eutrophication	METP	kg N eq.
Terrestrial Ecotoxicity	TECT	kg 1,4-DCB
Freshwater Ecotoxicity	FECT	kg 1,4-DCB
Marine Ecotoxicity	MECT	kg 1,4-DCB
Human Carcinogenic Toxicity	HCT	kg 1,4-DCB
Human Non-Carcinogenic Toxicity	HNCT	kg 1,4-DCB
Land use	LU	m^{2}a crop eq.
Mineral Resource Scarcity	MRS	kg CU eq.
Fossil Resource Scarcity	FRS	kg oil eq.
Water Consumption	WC	m^3

perspective) is employed for impact assessment (Huijbregts et al., 2017). This approach was chosen due to its comprehensive coverage of 18 environmental impact categories (Table 3), its precautionary principle approach that accounts for all potential impact pathways, and its conservative nature in environmental impact estimation (Huijbregts et al., 2016). This method is particularly well-suited to the PSC production system under study, as the selected impact categories effectively capture the dominant environmental burdens associated with the manufacturing processes described in previous sections.

Given that several production steps involve high-temperature processes, significant energy consumption is anticipated. Consequently, environmental impact categories directly associated with energy use were included in the assessment. Since the electricity grid mix remains predominantly fossil fuel-based, key impact categories such as global warming from CO_2 emissions, eutrophication and acidification from SO_x and NO_x emissions, and fine particulate matter formation were considered. In addition, the use of rare and toxic raw materials, such as lead and silver, necessitated the inclusion of resource scarcity impacts (mineral and fossil resource scarcity) and toxicity-related categories. Moreover, the ReCiPe 2016 midpoint (egalitarian) method was selected for its comprehensive coverage of these critical impact pathways and its widespread adoption in LCA research, including endorsement by the European Union's Joint Research Centre (Fazio et al., 2018; Hauschild et al., 2011; Pant et al., 2019). All calculations were performed using SimaPro™ v9.5.0.1 (PhD version) to ensure consistency with established LCA modelling practices.

3.2. Cumulative energy demand

The cumulative energy demand (CED) is one of the most widely used indicators for assessing the sustainability of PV technologies, as highlighted in previous studies (Li et al., 2022a; Frischknecht et al., 2005). This metric quantifies the total energy consumption throughout the entire life cycle of a system, offering a comprehensive perspective on the energy invested in the production of PSCs relative to the energy they generate. CED is measured in megajoules of primary energy (MJ eq.), encompassing both direct energy inputs (*e.g.*, electricity and thermal energy) and indirect contributions (*e.g.*, the embodied energy of materials) (Maranghi et al., 2019). The calculations were conducted using the CED method in SimaPro™ v9.5.0.1 (PhD version), ensuring consistency with established LCA modelling practices.

3.3. Energy analysis: energy payback time and energy return on investment

The EPBT and EROI are two key metrics for evaluating the energy performance of PSCs. EPBT (year) quantifies the time required for a PSC to generate an amount of energy equivalent to that consumed during its production. It is determined using the following equation (Celik et al., 2018):

$$\mathrm{EPBT} = \frac{E_{in}}{E_{out}} \tag{4}$$

where E_{in} (MJ/m^2) represents the primary energy demand of the PSC, encompassing both the embodied energy of materials and the direct energy required for processing. E_{out} (MJ/m^2) corresponds to the annual energy generated by the solar device, which is estimated using equation (5) (Celik et al., 2018):

$$E_{out,t} = I \times PCE_t \times PR \times \varepsilon \tag{5}$$

where I (MJ/m^2 year) is the annual solar irradiation, PCE_t (%) is the power conversion efficiency of the PSC for time t, PR is the performance ratio accounting for system losses, and ε (%) represents the energy-to-electricity conversion efficiency factor. Although ε varies depending on the selected grid, an average value of 31 % is assumed for Europe. (Celik et al., 2018; Yue et al., 2014)

The EROI is a dimensionless metric that quantifies the ratio of the total energy generated by a PSC over its lifetime to the energy invested in its production. It is determined using equation (6) (Celik et al., 2018):

$$\mathrm{EROI} = \frac{LT}{\mathrm{EPBT}} \tag{6}$$

where LT (year) represents the expected lifetime of the PSC, and EPBT (year) is the energy payback time, as defined in equation (4).

3.4. Economic analysis: levelized cost of electricity

The LCOE is a key economic metric for evaluating the feasibility of PV systems. It is calculated as the total life cycle cost divided by the total energy generated over the system's lifetime (Llanos et al., 2020). In this study, LCOE is expressed in €/kWh.

To determine the LCOE, it is essential to estimate the total energy output of the PSC over its economic lifetime, assess the investment costs and divide the life cycle cost by the total energy generated by the PSC (Hadi and Heidari, 2021); this calculation is expressed using equation (7) (Branker et al., 2011):

$$\mathrm{LCOE} = \frac{\sum_{t=0}^{LT} \frac{C_t}{(1+r)^t}}{\sum_{t=0}^{LT} \frac{E_t}{(1+r)^t}} \tag{7}$$

where r (%) is the discount rate, t is the year of operation, C_t (€) is the total cost of the system during all lifetime and E_t (kWh) is the annual energy generated by the PSC. The discount rate must be estimated based on the country-specific conditions. (Hadi and Heidari, 2021) For Portugal, a 7 % discount rate was assumed. (Trinomics BV Energy costs, 2020)

The C_t can be estimated using equation (8) (Branker et al., 2011):

$$C_t = I_t + O_t + M_t \tag{8}$$

where I_t (€) is the initial investment cost, O_t (€) is the operating cost for time t and M_t (€) is the maintenance cost for time t. The initial investment cost includes material and energy costs. Material costs were estimated based on 2024 retail prices and the required material quantities for producing a single PSC at lab-scale. The energy cost was assumed to be 0.10 €/kWh. (Energias de Portugal, 2023) Annual operation and maintenance costs were considered to be 10 % and 5 %, respectively, of the initial investment cost.

Disposal costs of the non-recycled materials were not included in this study, as the system was assessed at a small scale. Nevertheless, for the chosen scenario (incineration with energy recovery and flue gas cleaning), estimated costs in Europe range between 330 € and 630 € per tonne, depending on factors such as country, landfill class and taxes (Frederik Neuwahl et al., 2019; Steinmüller Babcock Environment; Lima and Bachmann, 2002). Exploring alternative disposal or recycling strategies could help minimize these costs and further improve the environmental and economic performance of the system.

3.5. Sensitivity analysis

The results of the LCA are highly dependent on the assumptions made throughout the study. After establishing the baseline scenario, a sensitivity analysis was performed to assess the influence of key parameters on the energy and economic performance of the PSC, specifically its lifetime, PCE and degradation rate. Given that the energy output of a PV system is strongly influenced by solar irradiance and climate conditions, the study considered multiple geographic locations across Europe with diverse climates, including Norway, Finland, Poland, France, Greece and Spain. Additionally, the analysis examined the

impact of replacing the Portuguese electrical mix with those of France, Germany, Greece, or Poland, as well as the implications of transitioning to a fully renewable electricity mix in these countries. The sensitivity analysis serves as a valuable tool for identifying opportunities for optimization and guiding future improvements.

4. Results and discussion

4.1. Environmental impact assessment – baseline scenario

In this section, the results of the LCA for the baseline scenario are presented, with the corresponding inputs and assumptions considered summarized in Table 4.

4.1.1. Life cycle inventory

The material and energy requirements per functional unit are shown in Table 5. The environmental impacts were calculated for each individual layer, with the inventory organized according to each layer deposition step. Given the small scale of the PSC under study, the materials consumed to produce it are relatively small.

4.1.2. Energy inventory

The direct processing energy was estimated for each production step of the solar cell, as shown in Table 5. The total energy required for producing the investigated inverted PSC was calculated to be 0.13 kWh/cm^2, a value that exceeds the previously reported estimates of 0.11 kWh/cm^2 [(Espinosa et al., 2015)] and 0.015 kWh/cm^2 (Guerrero et al., 2021). Nevertheless, this value remains justified, as the structure investigated here is more efficient than those reported in earlier studies.

As shown in Fig. 3, which illustrates the relative energy contribution of various steps in the PSC production process, the deposition of the silver back-contact accounts for the highest energy consumption. This outcome is expected, as the process involves thermal evaporation under high-vacuum conditions, which is inherently energy-intensive. To reduce energy consumption of this stage, several strategies could be considered, such as adopting more energy-efficient equipment, modifying the deposition technique, or substituting materials. For example, replacing silver with aluminium or using carbon paste applied via doctor-blading may offer significant energy savings.

4.1.3. Cradle-to-grave environmental impacts of the PSC

Fig. 4 presents the environmental impact values per FU for the baseline scenario, in which the energy used for PSC production is assumed to be supplied by the Portuguese electricity mix. As noted in the description of PSC Operation (in section 3.1.2), the environmental impacts of the utilization phase were considered negligible. The absolute values for each environmental impact category are provided in Supplementary data (Table S21). Since the magnitudes of these impacts vary across several orders, the data were scaled to enable visualization within a single graph with a comparable range across all categories. The results indicate that the production phase overwhelmingly dominates the overall performance of the PSC. Furthermore, the implemented strategy to recycle the FTO-glass substrate (previously described in the PSC End-of-life Scenario in section 3.1.2) was found to have a relatively low environmental impact. This strategy should be improved to help reduce both production costs and waste generation. Its environmental benefits could be further enhanced by incorporating a process for recycling the noble metal used in the back-contact. From a cradle-to-grave perspective under the specified conditions, a carbon footprint of 0.20 kg CO_2 eq./kWh was determined. Fig. 5 shows the contribution of each process step, highlighting the thermal deposition of the silver back-contact as the most significant contributor. The remaining steps each contribute less than 7 % to the total impact, indicating that future efforts to reduce the PSC's carbon footprint should prioritize the development of more sustainable materials and/or less energy-intensive deposition techniques for the back-contact.

Table 4
– Summary of the inputs and assumptions considered for the baseline scenario.

Parameter	Value
Power conversion efficiency	18.8 %
Lifetime	5 years
Degradation rate	4 %/year
Area	1 cm^2
Coordinates of the laboratory site (FEUP, Portugal)	41° 10′ 40.8″ N, 8° 35′ 49.2″ W
Average annual irradiation (based on the defined above location)	1897.32 kWh/m^2
Performance ratio	75 %
Energy-to-electricity conversion efficiency factor	31 %
Discount rate	7 %

4.1.4. Cradle-to-grave environmental impacts of embedded materials

Fig. 6 illustrates the relative contribution of the embedded materials (excluding energy consumption) per FU across various environmental impact categories, by deposition step. The absolute values of the environmental impacts for each impact category can be found in the Supplementary data (Table S22). The back-contact layer dominates the impact categories Mineral Resource Scarcity (MRS), Human Carcinogenic Toxicity (HCNT), Marine Ecotoxicity (MECT), and Freshwater Ecotoxicity (FECT). Due to the environmental burden associated with mineral extraction of silver, it also contributes significantly to other impact categories. The ETL is the primary contributor to Human Non-Carcinogenic Toxicity (HCN) impacts and a significant influence on the Ionizing Radiation (IR) category, mainly due to the production of PCBM, which involves toxic chemicals such as benzene, toluene, and sulfuryl chloride. Furthermore, the ETL contributes significantly to the Water Consumption (WC), Freshwater Eutrophication Potential (FETP), Fossil Resource Scarcity (FRS), and Global Warming (GW) categories, driven by the high steam and energy demands, primarily from fossil fuels, during PCBM production. The end-of-life stage has significantly impacted the Land Use (LU) and Stratospheric Ozone Depletion (SOD) categories, primarily due to the incineration of the hazardous waste. It also contributes to Water Consumption (WC) and Marine Eutrophication Potential (METP) categories, due to the use of potassium hydroxide solution in the recycling of FTO-glass substrates.

4.1.5. Cradle-to-grave environmental impacts of each process step

Fig. 7 presents the cradle-to-grave environmental impacts per FU for each production step of the inverted PSC under study. The absolute values can be found in the Supplementary data (Table S24). The figure clearly demonstrates that the deposition of the silver back-contact dominates all environmental impact categories, accounting for over 70 % of the total impacts. This dominance is primarily attributed to the energy required for this step, which involves thermal evaporation under high-vacuum conditions, emphasizing energy consumption as a key environmental factor. The deposition of the perovskite layer also significantly influences all environmental impact categories, because of the inclusion of lead and other organic and inorganic compounds in its composition. Despite the toxicity of these compounds, only small quantities are required to fabricate the thin films. Additionally, the cleaning of the FTO-glass substrate substantially impacts all categories, contributing approximately 5 % to the total impacts, highlighting the need for improvements in this process. It is important to note that the energy required for each step is the primary driver behind the observed impact distribution, as only small amounts of material are used in the production of the deposited thin films.

4.2. Cumulative energy demand – baseline scenario

Table 6 presents the total CED per FU output for the studied PSC. The data show that 4.67 MJ/kWh is required for the production phase, while

Table 5
– Life cycle inventory results per functional unit (kWh) for the production of a lab-scale inverted PSC.

Step	Sub-step	Material/ Equipment	Amount	Unit	Comments
FTO glass preparation	FTO-coated glass identification	FTO glass	1.31×10^{-1}	g/FU	
		VersaLaser	5.17×10^{-5}	kWh/ FU	Energy consumed
	FTO-coated glass etching	FTO glass	1.31×10^{-1}	g/FU	
		VersaLaser	2.02×10^{-5}	kWh/ FU	Energy consumed
	FTO-coated glass cleaning	FTO glass	1.31×10^{-1}	g/FU	
		Deionised water	4.86×10^{-1}	g/FU	Materials used in the cleaning process
		Acetone	3.82×10^{-1}	g/FU	
		2-propanol	3.81×10^{-1}	g/FU	
		Ultrasonic bath	4.05×10^{-4}	kWh/ FU	5 min with deionised water +10 min with acetone +10 min with 2-propanol
		Drying	1.14×10^{-8}	kWh/ FU	Drying 5 s with N_2 flow
		Oxygen plasma	9.78×10^{-4}	kWh/ FU	10 min of oxygen plasma treatment
HTL deposition		PTAA	6.07×10^{-6}	g/FU	Preparation of the HTL solution
		Toluene	3.51×10^{-3}	g/FU	
		Spin-coater	4.50×10^{-4}	kWh/ FU	Energy consumed during the deposition and sintering process of the HTL
		Hot plate	6.75×10^{-4}	kWh/ FU	
F-PEAI interlayer deposition		F-PEAI	4.05×10^{-5}	g/FU	Preparation of the interlayer solution
		DMF	7.69×10^{-3}	g/FU	
		Spin-coater	3.37×10^{-4}	kWh/ FU	Energy consumed during the deposition of the interlayer
Perovskite layer deposition	Triple cation perovskite precursor solution	PbI_2	2.51×10^{-3}	g/FU	Preparation of the triple cation perovskite precursor solution
		$PbBr_2$	3.21×10^{-4}	g/FU	
		FAI	8.52×10^{-4}	g/FU	
		MABr	9.79×10^{-5}	g/FU	
		CsI	7.57×10^{-5}	g/FU	
		DMF	3.69×10^{-3}	g/FU	
		DMSO	1.28×10^{-3}	g/FU	
	Anti-solvent solution	F-PEAI	1.01×10^{-6}	g/FU	Preparation of the anti-solvent solution
		Chlorobenzene	8.09×10^{-3}	g/FU	
		2-propanol	6.36×10^{-4}	g/FU	
		Spin-coater	4.39×10^{-4}	kWh/ FU	Energy consumed during the deposition and sintering process of the perovskite layer
		Hot plate	2.02×10^{-3}	kWh/ FU	
ETL deposition		PCBM	8.10×10^{-5}	g/FU	Preparation of the ETL solution
		Chlorobenzene	4.49×10^{-3}	g/FU	
		Spin-coater	3.37×10^{-4}	kWh/ FU	Energy consumed during the deposition and sintering process of the ETL
		Hot plate	6.75×10^{-4}	kWh/ FU	
Buffer layer deposition		BCP	2.02×10^{-6}	g/FU	Preparation of buffer layer solution
		2-propanol	3.18×10^{-3}	g/FU	

(*continued on next page*)

Table 5 (*continued*)

Step	Sub-step	Material/ Equipment	Amount	Unit	Comments
		Spin-coater	3.37×10^{-4}	kWh/ FU	Energy consumed during the deposition of the buffer layer
Back-contact deposition		Ag	2.02×10^{-3}	g/FU	Amount of silver deposited in 1 PSC
		Thermal evaporator	2.33×10^{-2}	kWh/ FU	Energy consumed during the thermal evaporation of silver

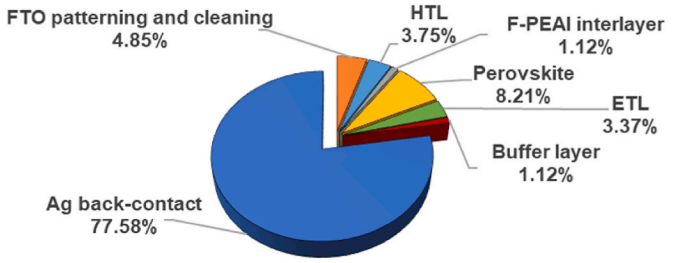

Fig. 3. – Energy consumption per layer deposition step to produce a lab-scale inverted PSC.

0.206 MJ/kWh is associated with the end-of-life stage. The table also indicates that approximately 68 % of the energy consumed during production is sourced from non-renewable energy sources, with the remaining 32 % coming from renewable sources. A similar distribution is observed during the end-of-life stage, where 65 % of the energy originates from non-renewables, and 35 % from renewables. Given that renewable energy sources generally have a lower environmental impact than non-renewables, increasing their share in the energy mix could significantly enhance the overall environmental performance of PSCs.

4.3. Energy analysis: energy payback time and energy return on investment – baseline scenario

To estimate the energy generated by the PSC, the annual average irradiation in Porto (1897.32 kWh/m^2) was used, as determined by the open access PVGIS web tool (Huld et al., 2012). Assuming a 5-year lifetime, a PCE of 18.8 % and a degradation rate of 4 %/year, the PSC is expected to generate approximately 12.35 kWh. The EPBT was calculated using equation (4), and its evolution over the device's lifetime is presented in Table 7. The inverted PSC system analysed in this study requires approximately 0.53 years to recover the energy consumed throughout its life cycle. The EPBT values reported in the literature for perovskite-based devices vary significantly, as summarized in Table 8.

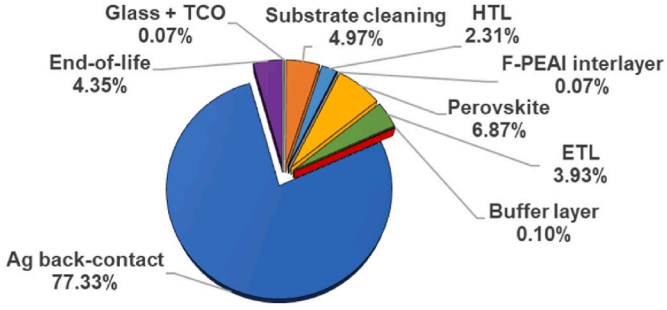

Fig. 5. – Contribution of each process step to the carbon footprint of the PSC.

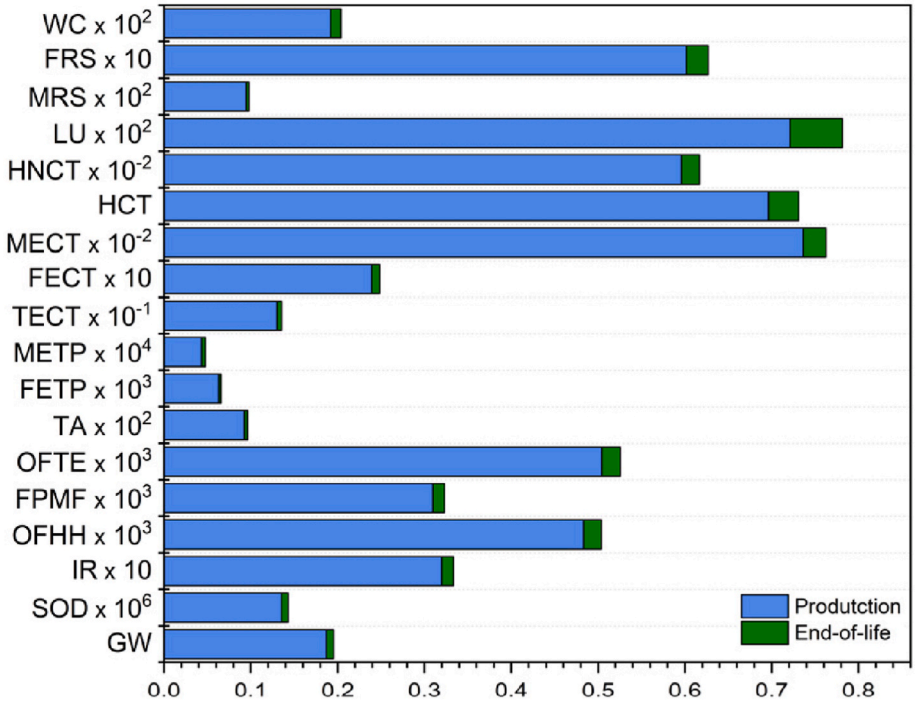

Fig. 4. – Cradle-to-grave environmental impacts of the inverted PSC.

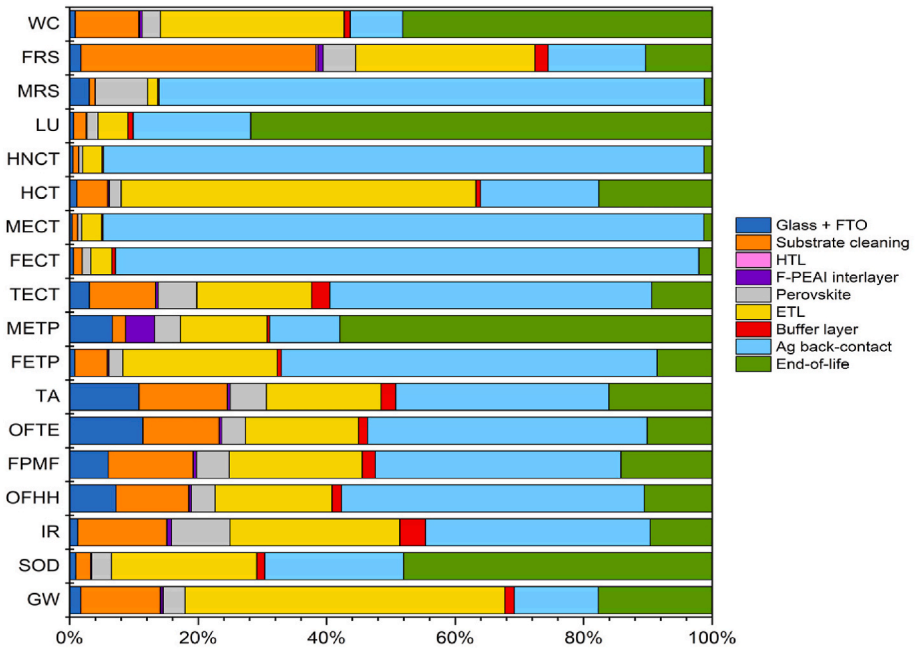

Fig. 6. – Relative distribution of environmental impacts across each step in the cradle-to-grave life cycle of the materials for the system under study.

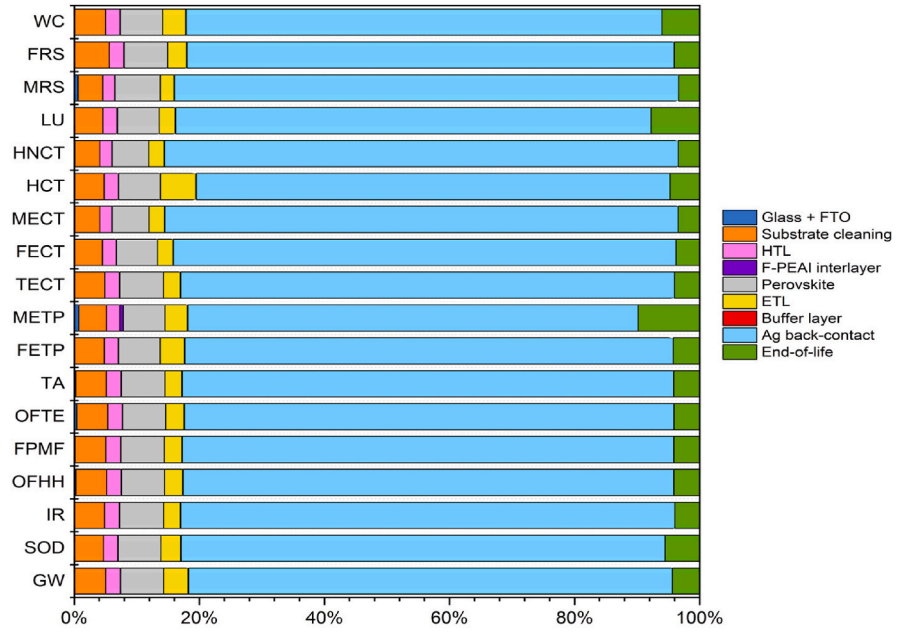

Fig. 7. – Relative distribution of environmental impacts across each step in the cradle-to-grave life cycle for the system under study.

Table 6
– Cradle-to-grave energy requirements of the inverted PSC calculated with CED method.

Impact category	Unit	Production	End-of-life
Non-renewable, fossil	MJ/kWh	2.76	1.17×10^{-1}
Non-renewable, nuclear	MJ/kWh	4.21×10^{-1}	1.73×10^{-2}
Non-renewable, biomass	MJ/kWh	3.45×10^{-5}	3.13×10^{-5}
Renewable, biomass	MJ/kWh	1.38×10^{-1}	1.74×10^{-2}
Renewable, wind, solar, geothermal	MJ/kWh	8.75×10^{-1}	3.54×10^{-2}
Renewable, water	MJ/kWh	4.74×10^{-1}	1.93×10^{-2}
Total	MJ/kWh	4.67	2.06×10^{-1}

Table 7
– Variation of EPBT and EROI values with the lifetime for the PSC under study (18.8 % PCE and degradation rate of 4 %/year operating in Porto).

Lifetime (year)	EPBT (year)	EROI
1	0.45	2.24
2	0.47	4.30
5	**0.53**	**9.50**
10	0.65	15.5
15	0.79	19.0
20	0.97	20.6
25	1.19	21.0

Table 8
– Values of EPBT reported in the literature.

Ref.	Architecture	Annual irradiation (kWh/m^2 year)	PCE (%)	Lifetime (year)	EPBT (year)
This study	Inverted	1897.32	18.8	5	0.53
Espinosa et al. (2015)	Regular	1700.0	15.4	1	17.3
			15.4	15	1.15
Gong et al. (2015)	Regular	1700.0	11.0	2	0.22-0.27
			9.10		
Celik et al. (2016)	Regular	1700.0	15.0	5	1.0-1.5
Sarialtin et al. (2020)	Regular	1700.0	14.5	5	0.58-0.74
			11.5		
Guerrero et al. (2021)	Regular	1530.0	15.0	4.3	0.83
Rao et al. (2021)	Regular	1513.5	18.0	3	0.97
Espinosa et al. (2015)	Inverted	1700.0	11.5	1	16.5
				15	1.10
Guerrero et al. (2021)	Inverted	1530.0	19.0	4.3	0.67
Okoroafor et al. (2022)	Inverted	850.0	11.4	20	2.17

The value obtained in this study ranks among the lowest, highlighting the strong energetic viability of the inverted PSC structure. A 2021 review by Vidal et al. (2021) reported a mean EPBT of 0.66 years for lab-scale PSCs, further supporting the results presented here.

Using the EPBT values and equation (6), the EROI was calculated to determine the minimum duration required for the PSC to recover the invested energy (see Table 7). As shown, a positive energy balance is achieved within the first year, with an EROI greater than 1. Furthermore, based on the work by Raugei et al. (2017), which reported EROI values for PV systems in Switzerland – conditions closely approximating those in Porto – the system analysed in this study falls within the reported range of 9.10 to 9.70, with an EROI value of 9.50.

The results in Table 7 indicate that EPBT and EROI vary with the assumed device lifetime. A slight increase in EPBT is observed as the lifetime increases, which may appear counterintuitive at first glance. This behaviour results directly from the modelling assumptions adopted in this study. Specifically, the energy input (E_{in}) was considered constant, as it represents the one-time energy investment associated with the manufacturing of the PSC, while the energy output (E_{out}) was calculated by accounting for a constant annual degradation rate of 4 %. Under these conditions, the electricity generated in each additional year of operation becomes progressively smaller due to the cumulative effect of degradation. Consequently, the marginal increase in total energy output diminishes over time. This leads to a gradual increase in EPBT for longer lifetimes, as the marginal energy gains in later years become progressively smaller due to cumulative degradation.

It should be noted that the lifetime values beyond the baseline scenario (5 years) are included as part of a parametric sensitivity analysis and are not intended to represent physically consistent operating conditions under a constant degradation rate of 4 %/year. In practice, such a degradation rate would limit the achievable lifetime according to standard T_{80} definitions. Therefore, lifetime and degradation rate are treated as independent parameters in this analysis to isolate their individual effects on system performance.

Despite the observed increase in EPBT, extending the device lifetime remains beneficial from an overall sustainability perspective. Longer lifetimes allow for greater cumulative electricity generation, which contributes to reducing the environmental impacts per functional unit and improving the economic performance of the technology.

This study also analysed the EPBT for a regular PSC architecture with the following structure: glass/FTO/c-TiO_2/m-TiO_2/$Cs_x[(CH_3(NH_2)_2)_{1-y}(CH_3NH_3)_y]_{1-x}Pb(I_{1-z}Br_z)_3$/spiro-OMeTAD/Au. Detailed information on the production process of this architecture is available in the work by Mesquita et al. (2019). The key difference in the fabrication process of the n-i-p PSC, compared to the p-i-n PSC, lies in the energy-intensive thermal treatment required during the deposition and sintering of the ETL. The LCI data for the regular PSC is provided in the Supplementary data (Table S25). The total energy consumption for producing an n-i-p PSC was calculated to be 0.41 kWh/cm^2.

Fig. 8 shows the relationship between EPBT and PCE for both p-i-n and n-i-p PSC architectures operating in Porto, Portugal, assuming a lifetime of 5 years and a degradation rate of 4 %/year for both architectures. As expected, the EPBT decreases as the PCE increases, with the values for 18.8 % efficiency represented by a red dot for both architectures. The results show that the p-i-n architecture consistently exhibits lower EPBT values, meaning it requires less time to recover the energy invested in its production. This translates into both environmental and economic benefits. Moreover, an asymptotic behaviour is observed as PCE increases, suggesting that beyond a certain point, further improvements in cell efficiency yield diminishing returns in terms of energy payback.

4.4. Economic analysis: levelized cost of electricity – baseline scenario

To further analyse the inverted PSC under study, an economic evaluation of its production and use was conducted. As previously mentioned, material costs were estimated based on 2024 retail prices and the quantity of materials required to produce a single lab-scale PSC (see Table 9 for detailed information), while the energy cost was assumed to be 0.10 €/kWh (Energias de Portugal, 2023). The total material and energy costs for producing the inverted PSC with the studied structure were determined to be 0.66 €/cm^2 and 0.01 €/cm^2, respectively, resulting in a total production cost of 0.67 €/cm^2.

Fig. 9 shows the relative distribution of material and energy costs for each layer of the PSC. This figure reveals that approximately 44 % of the material costs are attributable to the reagents used in the ETL, in particular PCBM and chlorobenzene, which together account for nearly half of the total material costs. To reduce the overall cost, substituting these compounds is recommended. The second largest contributor to material costs is the perovskite layer, accounting for approximately

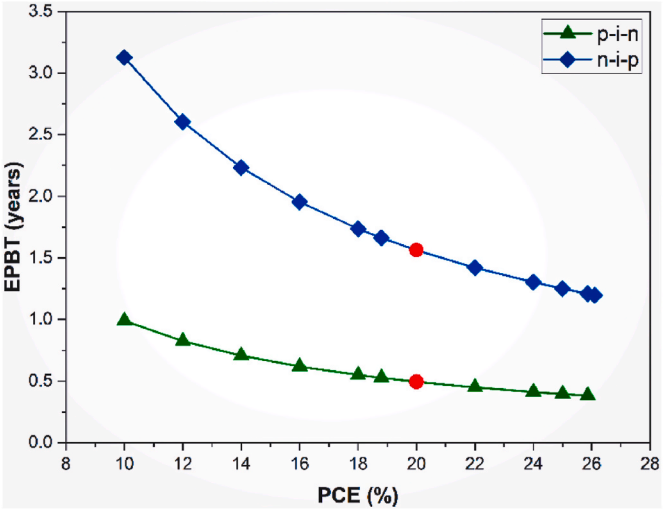

Fig. 8. – Variation of the EPBT value with the PCE for both n-i-p and p-i-n architectures (PSCs with a 5-year lifetime and a degradation rate of 4 %/year operating in Porto).

Table 9
– Retail prices in 2024 and quantity of materials required to produce an inverted PSC with 1 cm^2 of active area.

Material	Supplier	Cost	Amount per cell
2-Propanol	VWR	20.73 €/2.5 L	6.0 mL
2-Propanol, anhydrous	Sigma-Aldrich	65.10 €/100 mL	60 µL
F-PEAI	TCI Europe N.V.	81.00 €/1 g	0.51 mg
PCBM	Ossila	782.00 €/1 g	1.0 mg
Acetone	VWR	13.41 €/5 L	6.0 mL
BCP	Sigma-Aldrich	269.0 €/500 mg	0.025 mg
CsI	Sigma-Aldrich	96.90 €/25 g	0.94 mg
Chlorobenzene, anhydrous	Sigma-Aldrich	128.0 €/250 mL	0.14 mL
DMSO, anhydrous	Sigma-Aldrich	98.60 €/100 mL	14 µL
FTO substrate	Greatcell Solar Materials	26.53 €/900 cm^2	2.9 cm^2
FAI	Greatcell Solar Materials	170.0 €/50 g	11 mg
$PbBr_2$	TCI Europe N.V.	68.00 €/5 g	4.0 mg
PbI_2	TCI Europe N.V.	251.0 €/25 g	31 mg
MABr	Greatcell Solar Materials	21.49 €/10 g	1.2 mg
DMF, anhydrous	Sigma-Aldrich	80.20 €/100 mL	0.15 mL
PTAA	Ossila	575.0 €/250 mg	0.075 mg
Ag	Kurt J. Lesker	136.0 €/50 g	25 mg
Toluene, anhydrous	Sigma-Aldrich	53.40 €/100 mL	50 µL

25 % of the total cost. This contribution was expected due to its relatively large thickness compared to other layers, indicating a higher material requirement.

Regarding energy costs, as expected, the thermal evaporation of the silver back-contact accounts for the majority (~78 %) of the energy cost, due to the energy-intensive nature of the process, as discussed earlier. The deposition of the perovskite layer accounts for approximately 8 % of the energy costs, with the 30-min sintering step accounting for the largest proportion of this percentage.

Table 10 presents the variation of the LCOE as a function of the PSC's lifetime. As shown, the LCOE generally decreases with increasing lifetime, as the initial investment is distributed over a larger amount of electricity generated. However, it is noteworthy that the influence of PCE diminishes at higher lifetime values, with the LCOE approaching a plateau for lifetimes exceeding 20 years. This behaviour can be explained by the progressive efficiency losses caused by PSC degradation. As the device operates over time, the cumulative degradation reduces the amount of electricity generated in later years. Consequently, the marginal gains in energy production decrease, and the total lifetime energy output grows at a slower rate. This leads to a reduced impact of lifetime extension on LCOE and, in some cases, a slight increase due to the decreasing efficiency in later stages of operation, as reflected in equation (7). For a 5-year lifetime, the calculated LCOE is 0.29 €/kWh. According to Vidal et al. (2021), PSCs would need to achieve a global weighted average LCOE of approximately 0.04 €/kWh to be competitive with commercial PV technologies. It is important to note that costs associated with encapsulation, wiring, and cabling were not included in this analysis. Moreover, this study considers a lab-scale PSC produced under non-optimized conditions. It is expected that, at an industrial scale, production processes will become more efficient and cost-effective, thereby reducing manufacturing costs and lowering the LCOE in accordance with its definition in equation (7).

4.5. Sensitivity analysis

4.5.1. Lifetime, PCE and degradation rate impact analysis

In this study, the environmental, energetic and economic impacts associated with the production of 1 kWh of electricity from an inverted PSC with an active area of 1 cm^2 were analysed. The baseline scenario relies on a set of key assumptions, including the PSC's lifetime, PCE, and degradation rate (see Table 4 for detailed information). This section presents a parametric sensitivity analysis, in which these parameters are varied independently in order to evaluate their influence on the results. This approach allows for the identification of the most critical drivers of environmental, energetic, and economic performance, while isolating the individual effect of each parameter.

Fig. 10 illustrates the influence of lifetime, PCE, and degradation rate on the GW impact, evaluated from a cradle-to-grave perspective. GW was selected as it is one of the most widely used and representative environmental indicators. Other impact categories exhibited similar qualitative trends. As shown in the figure, increasing the device's lifetime leads to a reduction in GW impact, highlighting the importance of device durability in improving environmental performance. However, GW values tend to approach a plateau at longer lifetimes due to performance losses associated with cumulative degradation. As degradation progresses, the additional electricity generated in later years becomes progressively smaller, reducing the marginal benefit of lifetime extension in terms of impact per kWh.

When compared with previously reported GW values for inverted PSCs, such as 5.24 kg CO_2 eq./kWh for a 1-year lifetime, 0.35 kg CO_2 eq./kWh for a 15-year lifetime (Espinosa et al., 2015; U.S. Energy Information Administration, 2025)0.55 ± 1.05 kg CO_2 eq./m^2 for a

Table 10
– Variation of LCOE value with the PSC's lifetime (18.8 % PCE and degradation rate of 4 %/year operating in Porto).

Lifetime (year)	LCOE (€/kWh)
1	0.87
2	0.50
5	**0.29**
10	0.23
15	0.21
20	0.22
25	0.22

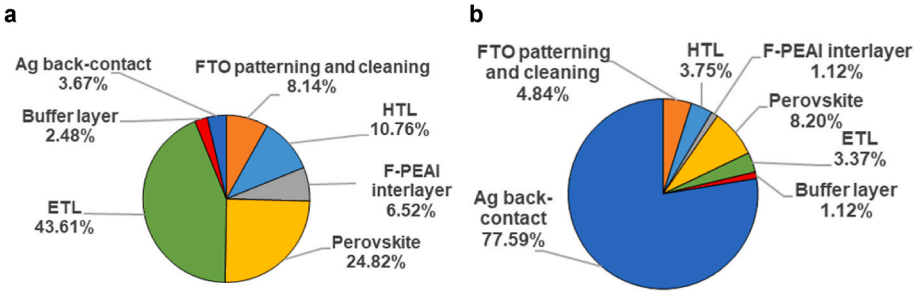

Fig. 9. – Relative distribution of the a) material and b) energy costs of each layer of the PSC.

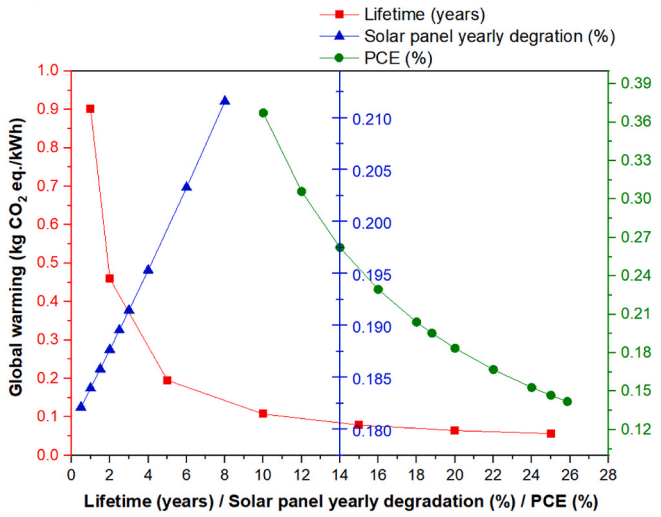

Fig. 10. – Variation of the GW impact with lifetime, PCE and degradation rate for a PSC operating in Porto. Note: The y-axis represents GW impact (kg CO_2 eq./kWh), while the x-axis corresponds explicitly to the parameter under analysis (PCE, lifetime, or degradation rate).

2-year lifespan (Li et al., 2022a), the device analysed in this work exhibits significantly lower impacts. Although some studies report GW values per unit area (*e.g.*, 9.55 ± 1.05 kg CO_2 eq./m^2 for a 2-year lifespan (Li et al., 2022a)), direct comparison remains indicative of the relatively low environmental burden of the system assessed here.

Fig. 10 also shows that higher PCE values lead to lower GW impacts due to increased electricity generation, whereas higher annual degradation rates result in higher GW impacts, as the reduced long-term electricity output increases the environmental impact per kWh.

The variation of EPBT, EROI and LCOE values as a function of the PSC lifetime were presented on Tables 7 and 10 for the base case scenario. However, these parameters are also highly sensitive to changes in PCE and degradation rate. Figs. 11 and 12 show how these parameters vary as a function of the values of PCE and degradation rate, respectively. Fig. 11 shows that, for the PSC under study to remain energetically viable, a minimum PCE of 18 % is required (corresponding to an EPBT of 0.53 and an EROI of 9.10), while the LCOE ranges from 0.21 to 0.54 €/kWh. Fig. 12 indicates that the maximum degradation rate a PSC can tolerate while maintaining energy viability is 5 % per year (with an EROI of 9.10), with the LCOE ranging from 0.26 to 0.32 €/kWh.

4.5.2. *Changing the energy country mix*

In this section it is analysed the influence of the electricity mix used in the PSC production. In particular, besides the Portuguese electricity mix considered in the base case scenario, the French, German, Greek or Polish mixes were also examined to identify which countries offer the most favourable conditions for producing and disposing of PSCs. The LCI information for each country energy mix was obtained from the ecoinvent v3.9.1 database. The values of the environmental impacts were determined for the production phase (Fig. 13a) and for the disposal phase (Fig. 13b), and the absolute values are provided in Tables S26 and S27 of the Supplementary data. The analysis reveals that Poland has the highest environmental impacts for both PSC production and disposal. This outcome was expected, given that Poland's electricity mix has the greatest impact per unit of energy generated due to its heavy reliance on fossil fuels, particularly coal (Iglinski et al., 2022), making it the least favourable option. Greece also exhibits significant environmental impacts, also because of its continued dependence on fossil fuels (International Energy Agency, 2023), despite its favourable condition for generating renewable electricity through PV panels. In contrast, France emerges as the most favourable country for PSC production and disposal across all categories, except for IR impact. This is due to the high share of nuclear power in the electricity mix (International Energy Agency, 2021), which, while being a low-carbon energy source, is associated with potentially higher impacts related to ionizing radiation. Given the geographical proximity between Portugal and France, a feasible strategy to further reduce the environmental impacts of the cradle-to-grave LCA of the PSC would be to produce the cells in France, closer to the markets of central Europe, and dispose of them in Portugal. However, although the Portuguese electricity mix is more renewable than the French one, legislative restrictions on PSC waste management may limit its advantages. Additionally, this analysis does not consider other important factors, such as supply chain constraints, which could restrict feasible options or significantly influence the actual

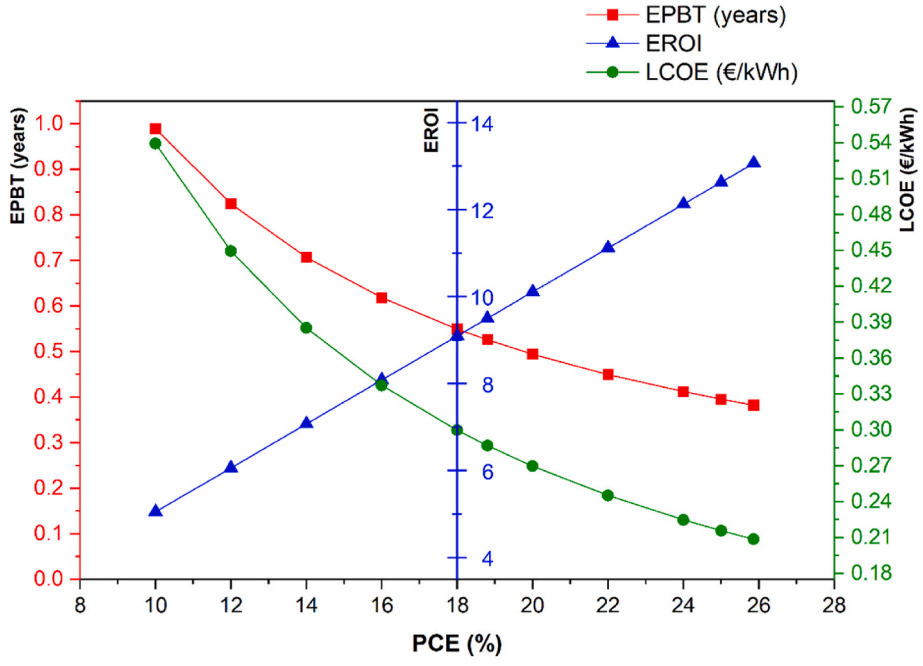

Fig. 11. – Variation of the EPBT, EROI and LCOE with the PCE (PSC with a 5-year lifetime and a degradation rate of 4 %/year operating in Porto).

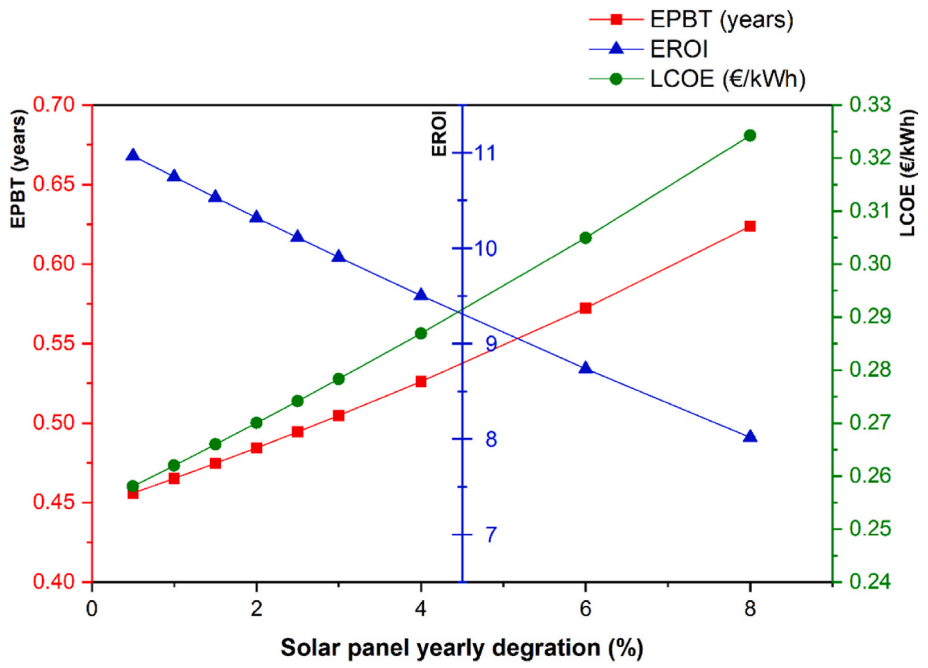

Fig. 12. – Variation of the EPBT, EROI and LCOE with the degradation rate (PSC with a 5-year lifetime and PCE 18.8 % operating in Porto).

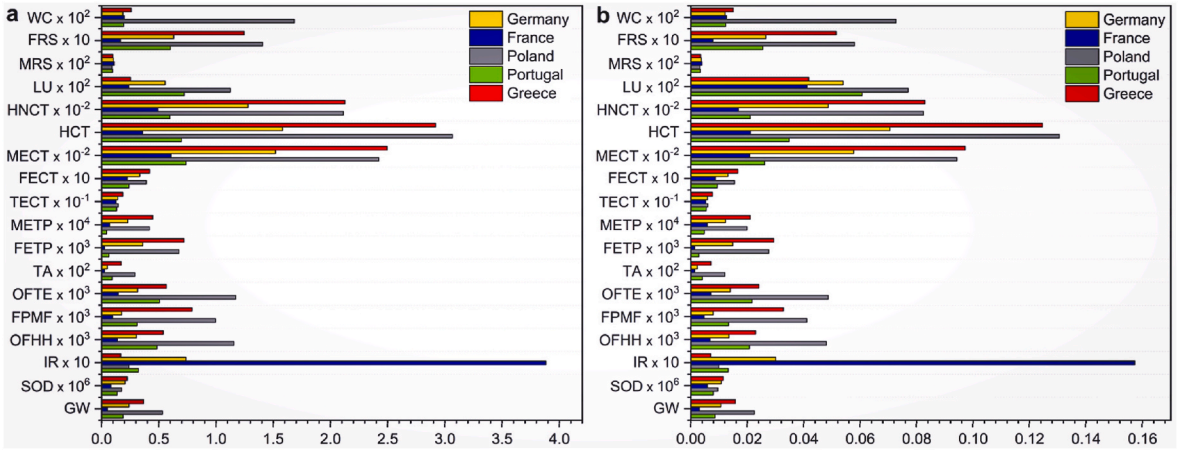

Fig. 13. – Environmental impacts resulting from the PSC a) production and b) disposal in several European countries.

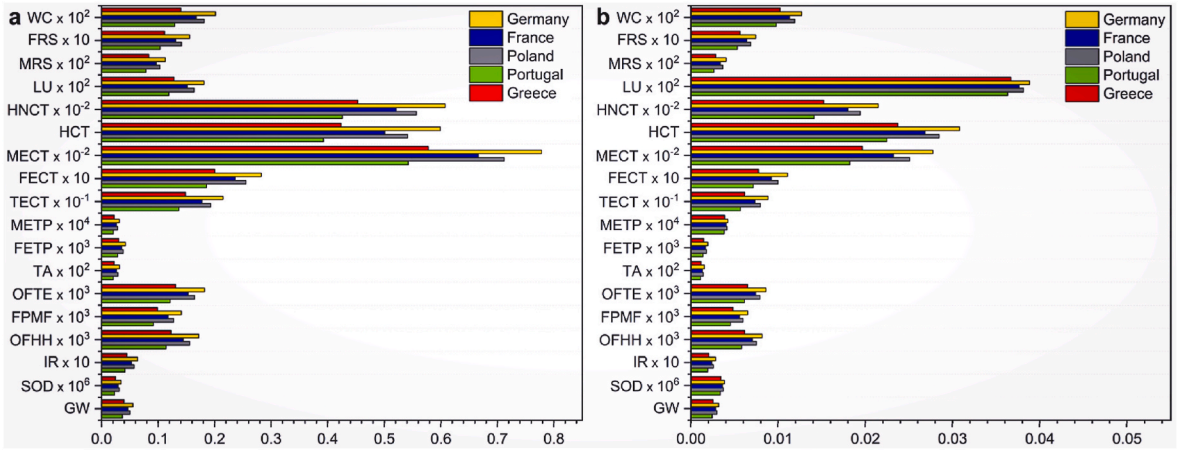

Fig. 14. – Environmental impacts resulting from the PSC a) production and b) disposal using the PV source in several European countries.

environmental performance of PSCs.

4.5.3. Changing the energy source (mix to fully renewable electricity)

The results presented above clearly indicate that the energy consumption associated with depositing the metallic back-contact is the primary factor influencing the environmental performance of the PSC. Therefore, efforts to reduce the environmental impacts should focus on this step, including transitioning from the current electricity mix, which still relies heavily on fossil fuels, to a fully renewable electricity mix sourced from PV silicon solar cells. This transition was modelled for the Portuguese, French, German, Greek and Polish electricity mixes, using the appropriate ecoinvent datasets. The results are shown in Fig. 14a for the production phase and Fig. 14b for the disposal phase (absolute values are provided in Tables S28 and S29 of the Supplementary data). Based on these findings, Portugal emerges as the most favourable country for both producing and disposing of the inverted PSC using PV energy, whereas Germany ranks as the least favourable.

When comparing the results presented in Fig. 14 with the results presented in Fig. 13, significant reductions across several environmental impact categories are observed. Fig. 15a and b illustrate the variation in environmental impacts associated with PSC production and disposal, respectively, when switching from the regular electricity mix to a fully renewable electricity mix sourced by PV panels. Absolute values are provided in Table S30 and Table S31 of the Supplementary data. For instance, for the French regular electricity mix, the IR impact category shows a reduction of over 98 % for both PSC production and disposal. Substantial decreases in GW potential were also observed for Germany, Poland, Portugal and Greece. However, it is notable that for France, more than half of the environmental impact categories exhibit increased impacts when transitioning from the regular electricity mix to the fully renewable PV-based electricity.

4.5.4. Generation of energy in different climate conditions

As previously mentioned, the PSC was produced in a laboratory at FEUP, Portugal, which according to the Köppen-Geiger climate classification (Peel et al., 2007), has a warm-summer Mediterranean climate (Csb). Since the energy generated by PV systems is highly sensitive to insolation conditions, which depend on the local climatic conditions, a sensitivity analysis was conducted considering various geographic locations across Europe with different climate conditions. Fig. 16 shows the locations analysed: Cantalejo (humid continental climate, dry cool summer – Dsb), Madrid (cold semi-arid climate – BSk), Almería (cold desert climate – BWk), Paris (temperate oceanic climate – Cfb), Finse (tundra climate – ET), Vaasa (subarctic with cool summers and year around rainfall – Dfc), Warsaw (humid continental mild summer, wet all year – Dfb) and Athens (hot-summer mediterranean climate – Csa). These locations exhibit significant variations in mean annual solar irradiation. Table 11 presents the geographical distribution of EPBT and EROI. As expected, locations with higher annual solar irradiation show lower EPBT values and higher EROI values. Therefore, climates classified as Csb, Dsb, Csa, BSk and BWk are more favourable for PV investments compared to climates classified as Dfc, Dfb, Cfb and ET.

Referring to the previously mentioned EROI range of 9.10 to 9.70 (Raugei et al., 2017), Table 11 shows that under the assumed conditions, not all the studied locations meet this threshold. Specifically, the locations with EROI values below 9.10 correspond to the climates previously identified as less attractive for PV investments (Dfc, Dfb, Cfb and ET, with low annual solar irradiation).

Regarding the variation in LCOE, although the threshold of 0.04 €/kWh (Vidal et al., 2021) is not meet, is possible to observe that there is an inverse relation between the obtained value and the annual solar irradiation: lower LCOE values are obtained in locations that present higher annual solar irradiations.

5. Conclusion

This study conducted a cradle-to-grave life cycle assessment on a lab-scale inverted PSC. As an emerging technology, PSCs have been the subject of limited comprehensive analyses regarding their environmental, energetic, and economic performance across production, operation, and disposal stages. The study found that producing the PSC requires a total energy input of 0.13 kWh/cm^2, with the thermal evaporation of the silver back-contact identified as the most energy-intensive step due to the high-vacuum conditions required. The carbon footprint was estimated at 0.20 kg CO_2 eq./kWh, with silver back-contact deposition dominating all environmental impact categories, accounting for over 70 % of total impacts. This is primarily attributed to both the high energy demand of this step and the environmental burden of silver extraction. From a cradle-to-grave perspective, the cumulative energy demand was 4.88 MJ/kWh, of which roughly 70 % originates from non-renewable energy sources and 30 % from renewable sources.

Energetically, the system requires approximately 0.53 years to recover the energy invested over its life cycle, achieving an energy return on investment of 9.50. These values position the studied PSC structure competitively relative to those reported in the literature. Economically, the production cost of the inverted PSC was estimated at 0.67 €/cm^2, with a levelized cost of energy of 0.29 €/kWh.

A sensitivity analysis highlighted that GW impact category is highly sensitive to the PSC's lifetime. PCE and degradation rate critically influence the system's energetic viability, while LCOE remains relatively stable across parameter variations. The optimal scenario combines longer lifetimes, higher PCEs, and lower degradation rates. Additionally,

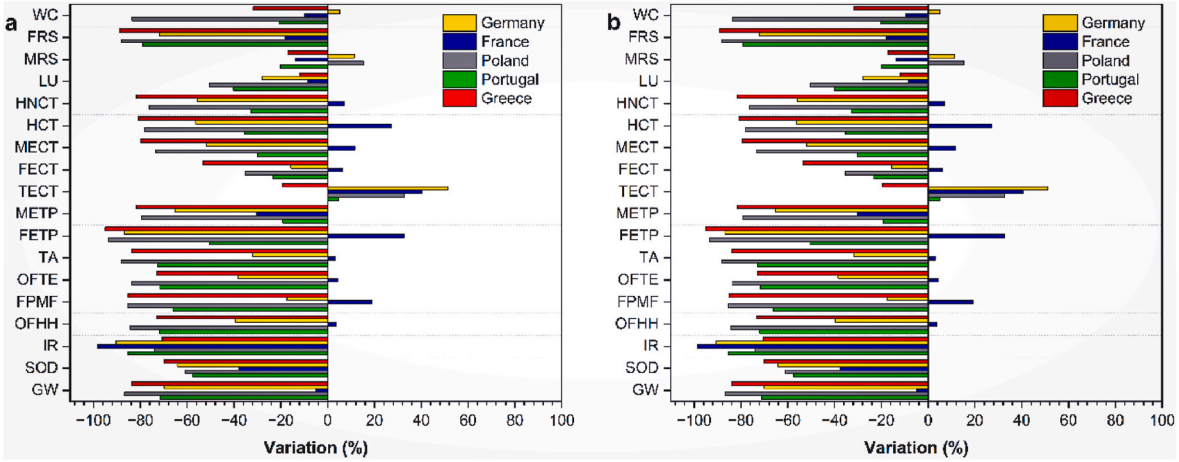

Fig. 15. – Variation of the environmental impacts of PSC a) production and b) disposal when changing from the electricity mix to the PV electricity.

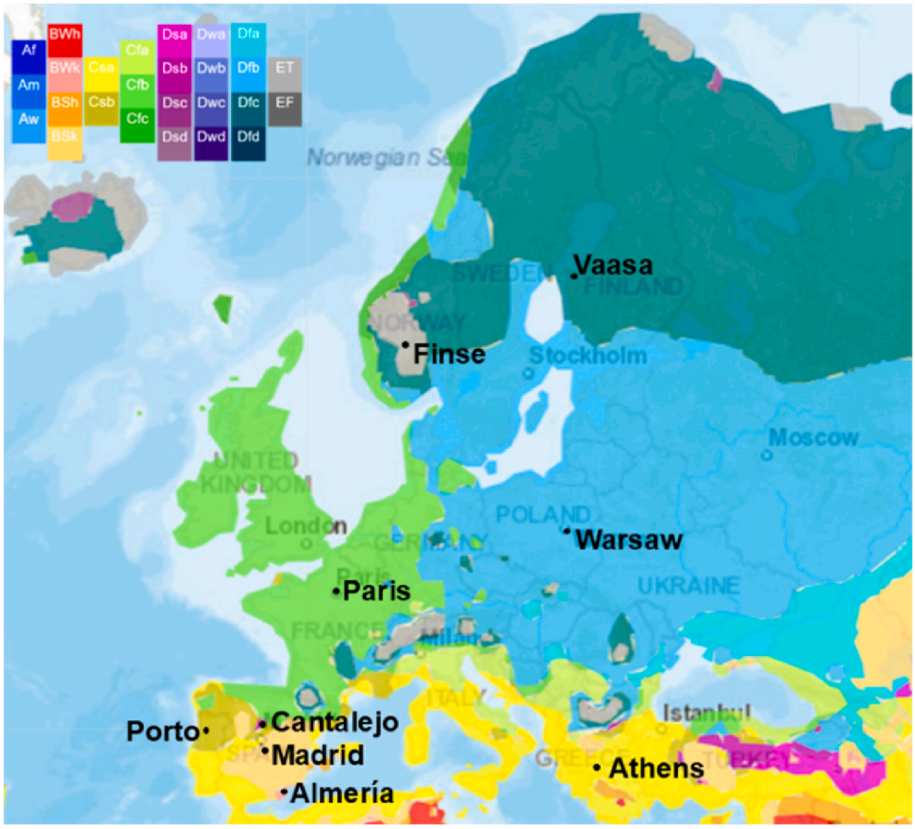

Fig. 16. – Köppen-Geiger climate type map of Europe. Adapted from ref. (PlantMaps, 2024).

Table 11
– EPBT, EROI and LCOE values calculated for different locations considering a PCE of 18.8 %, 5-year lifetime and a degradation rate of 4 %/year.

Location	Coordinates	Average annual irradiation (kWh/m^2 year)	Energy generated (kWh/lifetime)	EPBT (year)	EROI	LCOE (€/kWh)
Finse	60° 30′ 0″ N, 9° 5′ 60″ E	1110.05	7.22	0.90	5.56	0.49
Vaasa	63° 5′ 45.6″ N, 21° 36′ 57.6″ E	1205.33	7.84	0.83	6.04	0.45
Warsaw	52° 13′ 33.6″ N, 21° 0′ 14.4″ E	1310.80	8.53	0.76	6.57	0.42
Paris	48° 51′ 28.8″ N, 2° 21′ 10.8″ E	1425.19	9.28	0.70	7.14	0.38
Porto	41° 10′ 40.8″ N, 8° 35′ 49.2″ W	1897.32	12.3	0.53	9.50	0.29
Cantalejo	41° 14′ 49.2″ N, 3° 57′ 25.2″ W	1926.09	12.5	0.52	9.65	0.28
Athens	37° 58′ 51.6″ N, 23° 43′ 44.4″ E	2072.51	13.5	0.48	10.4	0.26
Madrid	40° 24′ 50.4″ N, 3° 42′ 21.6″ W	2101.20	13.7	0.48	10.5	0.26
Almería	36° 50′ 42″ N, 2° 28′ 48″ W	2177.94	14.2	0.46	10.9	0.25

EPBT and EROI are highly sensitive to local solar irradiation.

Although this LCA study focuses on a lab-scale PSC, the findings provide valuable insights for the research community regarding the environmental impacts associated with production and disposal of inverted PSC structure. The results can also guide future efforts to enhance the environmental, energetic and economic performance of these promising devices.

CRediT authorship contribution statement

Joana Príncipe: Conceptualization, Formal analysis, Investigation, Methodology, Software, Visualization, Writing – original draft. **Luísa Andrade:** Conceptualization, Funding acquisition, Resources, Supervision, Validation, Writing – review & editing. **Vera C.M. Duarte:** Writing – review & editing. **Teresa M. Mata:** Writing – review & editing. **António A. Martins:** Conceptualization, Methodology, Supervision, Validation, Writing – review & editing.

Declaration of competing interest

The authors declare that they have no known competing financial interests or personal relationships that could have appeared to influence the work reported in this paper.

Acknowledgments

This research work was supported by the doctoral grant (PRT/BD/152838/2021) of Joana Príncipe financed by the Portuguese Foundation for Science and Technology (FCT) and with funds from the State Budget, under the MIT Portugal Program (DOI: https://doi.org/10.54499/PRT/BD/152838/2021). This work was financially supported by the base funding of the following projects and entities: national funds through the FCT/MCTES (PIDDAC), under the project PTDC/EQU-EQU/4193/2021 (DOI: 10.54499/PTDC/EQU-EQU/4193/2021); national funds through FCT/MCTES (PIDDAC): LEPABE, UIDB/00511/2020 (DOI: 10.54499/UIDB/00511/2020) and UIDP/00511/2020 (DOI: 10.54499/UIDP/00511/2020) and ALiCE, LA/P/0045/2020 (DOI: 10.54499/LA/P/0045/2020); LAETA, UIDB/50022/2020 (DOI:

10.54499/UID/50022/2025); and CBQF, UID/50016/2025, LA/P/0076/2020 (DOI: 10.54499/LA/P/0076/2020). Vera C. M. Duarte thanks the funding of the project 2023.17945.ICDT with DOI 10.54499/2023.17945.ICDT (https://doi.org/10.54499/2023.17945.ICDT), funded by national funds through FCT/MECI. António Martins gratefully acknowledges the FCT, I.*P. and* the Recovery and Resilience Plan (PRR) of the Portuguese Republic, through the Recover Portugal Task Force, for funding under contract ref. 2023.15056.TENURE.038. Teresa Mata gratefully acknowledges the funding of project NORTE-06-3559-FSE-000107, cofinanced by Programa Operational Regional do Norte (NORTE2020), through Fundo Social Europeu (FSE).

Appendix A. Supplementary data

Supplementary data to this article can be found online at https://doi.org/10.1016/j.jclepro.2026.148924.

Data availability

Data will be made available on request.

References

Alberola-Borràs, J.A., Baker, J.A., De Rossi, F., Vidal, R., Beynon, D., Hooper, K.E.A., et al., 2018a. Perovskite photovoltaic modules: life cycle assessment of pre-industrial production process. iScience 9, 542–551. https://doi.org/10.1016/j.isci.2018.10.020.

Alberola-Borràs, J.A., Vidal, R., Juárez-Pérez, E.J., Mas-Marzá, E., Guerrero, A., Mora-Seró, I., 2018b. Relative impacts of methylammonium lead triiodide perovskite solar cells based on life cycle assessment. Sol. Energy Mater. Sol. Cells 179, 169–177. https://doi.org/10.1016/j.solmat.2017.11.008.

Alberola-Borràs, J.A., Vidal, R., Mora-Seró, I., 2018c. Evaluation of multiple cation/anion perovskite solar cells through life cycle assessment. Sustain. Energy Fuels 2, 1600–1609. https://doi.org/10.1039/c8se00053k.

Ardente, F., Eynard, U., Leccisi, E., Mathieux, F., Wolf, K., 2025. Harmonised Rules for the Calculation of the Carbon Footprint of Photovoltaic Modules in the Context of the EU Ecodesign Directive. European Commission.

Branker, K., Pathak, M.J.M., Pearce, J.M., 2011. A review of solar photovoltaic levelized cost of electricity. Renew. Sustain. Energy Rev. 15, 4470–4482. https://doi.org/10.1016/j.rser.2011.07.104.

Burnley, S., Wagland, S., Longhurst, P., 2019. Using life cycle assessment in environmental engineering education. High Educ. Pedagog. 4, 64–79. https://doi.org/10.1080/23752696.2019.1627672.

Carneiro, A.L., Martins, A.A., Duarte, V.C.M., Mata, T.M., Andrade, L., 2022. Energy consumption and carbon footprint of perovskite solar cells. Energy Rep. 8, 475–481. https://doi.org/10.1016/j.egyr.2022.01.045.

Celik, I., Mason, B.E., Phillips, A.B., Heben, M.J., Apul, D., 2017. Environmental impacts from photovoltaic solar cells made with single walled carbon nanotubes. Environ. Sci. Technol. 51, 4722–4732. https://doi.org/10.1021/acs.est.6b06272.

Celik, I., Philips, A.B., Song, Z.N., Yan, Y.F., Ellingson, R.J., Heben, M.J., et al., 2018. Energy Payback Time (EPBT) and Energy Return on Energy Invested (EROI) of perovskite tandem photovoltaic solar cells. IEEE J. Photovolt. 8, 305–309. https://doi.org/10.1109/Jphotov.2017.2768961.

Celik, I., Song, Z.N., Cimaroli, A.J., Yan, Y.F., Heben, M.J., Apul, D., 2016. Life Cycle Assessment (LCA) of perovskite PV cells projected from lab to fab. Sol. Energy Mater. Sol. Cells 156, 157–169. https://doi.org/10.1016/j.solmat.2016.04.037.

Chakraborty, K., Choudhury, M.G., Paul, S., 2021. Life cycle assessment of a lead-free cesium titanium (IV) single and mixed halide perovskite solar cell based 1 m2 PV module. IEEE Transact. Device Mater. Reliabil. 21, 465–471. https://doi.org/10.1109/Tdmr.2021.3106340.

Chaosukho, S., Meeklinhom, S., Rodbuntum, S., Sukgorn, N., Kaewprajak, A., Kumnorkaew, P., et al., 2024. Life cycle assessment of perovskite solar cells with alternative carbon electrode. Environ. Impact. Asses. 106, 107462. https://doi.org/10.1016/j.eiar.2024.107462.

Clegg, C., Mei, J.J., Fuensanta, A.U., Ibn-Mohammed, T., Pecunia, V., 2025. Evaluating lead-based vs. lead-free perovskites for environmentally sustainable indoor photovoltaics. Mater. Sci. Eng., R 166, 101037. https://doi.org/10.1016/j.mser.2025.101037.

Cuéllar-Franca, R.M., García-Gutiérrez, P., Taylor, S.F.R., Hardacre, C., Azapagic, A., 2016. A novel methodology for assessing the environmental sustainability of ionic liquids used for CO capture. Faraday Discuss. 192, 283–301. https://doi.org/10.1039/c6fd00054a.

Degani, M., An, Q., Albaladejo-Siguan, M., Hofstetter, Y.J., Cho, C., Paulus, F., et al., 2021. 23.7% efficient inverted perovskite solar cells by dual interfacial modification. Sci. Adv. 7, eabj7930. https://doi.org/10.1126/sciadv.abj7930.

Ember, 2024. Global Electricity Review. *2024*; May.

Energias de Portugal, 2023. ERSE announces electricity tariffs for 2024. https://www.edp.com/en/news/erse-announces-electricity-tariffs-2024 accessed June 2024.

Espinosa, N., Serrano-Luján, L., Urbina, A., Krebs, F.C., 2015. Solution and vapour deposited lead perovskite solar cells: ecotoxicity from a life cycle assessment perspective. Sol. Energy Mater. Sol. Cells 137, 303–310. https://doi.org/10.1016/j.solmat.2015.02.013.

European Commission, 2023. Renewable Energy Directive. https://energy.ec.europa.eu/topics/renewable-energy/renewable-energy-directive-targets-and-rules/renewable-energy-directive_en#directive-20182001eu. accessed November 2023.

European Environment Agency, 2025. Share of energy consumption from renewable sources in Europe. https://www.eea.europa.eu/en/analysis/indicators/share-of-energy-consumption-from accessed February 2026.

European Parliament, Council of the European Union, 2009. Directive 2009/28/EC of the European Parliament and of the Council of 23 April 2009 on the Promotion of the Use of Energy from Renewable Sources and Amending and Subsequently Repealing Directives 2001/77/EC and 2003/30/EC. Official Journal of the European Union, Strasbourg.

European Parliament, Council of the European Union, 2018. Directive 2018/2001 of the European Parliament and of the Council of 11 December 2018 on the Promotion of the Use of Energy from Renewable Sources. Official Journal of the European Union, Strasbourg.

Fazio, S., Castellani, V., Sala, S., Schau, E., Secchi, M., Zampori, L., et al., 2018. Supporting Information to the Characterisation Factors of Recommended EF Life Cycle Impact Assessment Methods: New Methods and Differences with ILCD. Publications Office of the European Union, Luxembourg.

Frederik Neuwahl, G.C., Gómez Benavides, Jorge, Holbrook, Simon, 2019. Serge Roudier *Best Available Techniques (BAT) Reference Document for Waste Incineration*. European Commission, Luxembourg.

Frischknecht, R., Heath, G., Raugei, M., Sinha, P., 2016. Wild-Scholten Md *Methodology Guidelines on Life Cycle Assessment of Photovoltaic Electricity*; IEA-PVPS T12-08:2016. International Energy Agency Photovoltaic Power systems Programme.

Frischknecht, R., Jungbluth, N., Althaus, H.J., Doka, G., Dones, R., Heck, T., et al., 2005. The ecoinvent database: overview and methodological framework. Int. J. Life Cycle Assess. 10, 3–9. https://doi.org/10.1065/lca2004.10.181.1.

Frischknecht, R., Stolz, P., Heath, G., Raugei, M., Sinha, P., 2020. Wild-Scholten Md *Methodology Guidelines on Life Cycle Assessment of Photovoltaic*. International Energy Agency.

Geisler, G., Hofstetter, T.B., Hungerbühler, K., 2004. Production of fine and speciality chemicals:: procedure for the estimation of LCIs. Int. J. Life Cycle Assess. 9, 101–113. https://doi.org/10.1007/Bf02978569.

Gong, J., Darling, S.B., You, F.Q., 2015. Perovskite photovoltaics: life-cycle assessment of energy and environmental impacts. Energy Environ. Sci. 8, 1953–1968. https://doi.org/10.1039/c5ee00615e.

Guerrero, N.B.C., Martínez, W.O.H., Civit, B., Perez, M.D., 2021. Energy performance of perovskite solar cell fabrication in Argentina. A life cycle assessment approach. Sol. Energy 230, 645–653. https://doi.org/10.1016/j.solener.2021.10.071.

Hadi, E., Heidari, A., 2021. Development of an integrated tool based on life cycle assessment, levelized energy, and life cycle cost analysis to choose sustainable facade integrated photovoltaic systems. J. Clean. Prod. 293, 126117. https://doi.org/10.1016/j.jclepro.2021.126117.

Hauschild, M., Goedkoop, M., Guinee, J., Heijungs, R., Huijbregts, M., Jolliet, O., et al., 2011. Recommendations for Life Cycle Impact Assessment in the European Context - Based on Existing Environmental Impact Assessment Models and Factors (International Reference Life Cycle Data System - ILCD Handbook). Publications Office of the European Union, Luxembourg.

He, S.S., Qiu, L.B., Ono, L.K., Qi, Y.B., 2020. How far are we from attaining 10-year lifetime for metal halide perovskite solar cells? Mater. Sci. Eng., R 140, 100545. https://doi.org/10.1016/j.mser.2020.100545.

Herrera, J.-P., Freeman, J., Ravilla, A., Celik, I., 2025. Evaluating the environmental impacts of various recycling approaches for perovskite solar cells. MRS Adv. 10, 1440–1446. https://doi.org/10.1557/s43580-025-01291-y.

Huber, E., Bach, V., Holzapfel, P., Blizniukova, D., Finkbeiner, M., 2022. An approach to determine missing life cycle inventory data for chemicals (RREM). Sustainability-Basel 14. https://doi.org/10.3390/su14063161.

Huijbregts, M.A.J., Steinmann, Z.J.N., Elshout, P.M.F., Stam, G., Verones, F., Vieira, M., et al., 2016. ReCiPe 2016: a Harmonized Life Cycle Impact Assessment Method at Midpoint and Endpoint Level - Report I: Characterization. National Institute for Public Health and the Environment, The Netherlands.

Huijbregts, M.A.J., Steinmann, Z.J.N., Elshout, P.M.F., Stam, G., Verones, F., Vieira, M., et al., 2017. ReCiPe2016: a harmonised life cycle impact assessment method at midpoint and endpoint level. Int. J. Life Cycle Assess. 22, 138–147. https://doi.org/10.1007/s11367-016-1246-y.

Huld, T., Müller, R., Gambardella, A., 2012. A new solar radiation database for estimating PV performance in Europe and Africa. Sol. Energy 86, 1803–1815. https://doi.org/10.1016/j.solener.2012.03.006.

Iglinski, B., Pietrzak, M.B., Kielkowska, U., Skrzatek, M., Kumar, G., Piechota, G., 2022. The assessment of renewable energy in Poland on the background of the world renewable energy sector. Energy 261, 125319. https://doi.org/10.1016/j.energy.2022.125319.

International Energy Agency, 2021. France 2021 - Energy Policy Review. IEA: France.

International Energy Agency, 2023. Greece 2023 - Energy Policy Review. IEA: France.

International Energy Agency, 2024. Electricity 2024 - Analysis and Forecast to 2026. IEA, France.

International Energy Agency, 2025. *Snapshot of Global PV Markets*; IEA-PVPS T1 - Strategic PV Analysis and Outreach. IEA.

ISO 14040, 2006. Environmental Management - Life Cycle Assessment - Principles and Framework. International Organization for Standardization.

ISO 14044, 2006. Life Cycle Assessment - Requirements and Guidelines. International Standard Organization.
Jech, Š., Hadadian, M., Miettunen, K., Santasalo-Aarnio, A., 2026. Revive or reuse: environmental and energy insights into mesoporous perovskite solar cells recycling. Sol. Energy Mater. Sol. Cells 302, 114315. https://doi.org/10.1016/j.solmat.2026.114315.
Jeng, J.Y., Chiang, Y.F., Lee, M.H., Peng, S.R., Guo, T.F., Chen, P., et al., 2013. CH3NH3PbI3 perovskite/fullerene planar-heterojunction hybrid solar cells. Adv. Mater. 25, 3727–3732. https://doi.org/10.1002/adma.201301327.
Jiang, K., Wu, F., Zhang, G.Y., Chow, P.C.Y., Ma, C., Li, S.F., et al., 2019. Inverted planar perovskite solar cells based on CsI-doped PEDOT:PSS with efficiency beyond 20% and small energy loss. J. Mater. Chem. A 7, 21662–21667. https://doi.org/10.1039/c9ta08995k.
Jiang, Q., Tong, J.H., Xian, Y.M., Kerner, R.A., Dunfield, S.P., Xiao, C.X., et al., 2022. Surface reaction for efficient and stable inverted perovskite solar cells. Nature 611, 278–283. https://doi.org/10.1038/s41586-022-05268-x.
Jordan, D.C., Kurtz, S.R., 2013. Photovoltaic degradation rates - an analytical review. Prog. Photovoltaic. 21, 12–29. https://doi.org/10.1002/pip.1182.
Kamali, A.K., Keppetipola, N.M., Yoshihara, Y., Jena, A.K., Uchida, S., Segawa, H., et al., 2024. Validating the "greenness" of chemicals via life cycle assessment: the case of anisole as an anti-solvent in perovskite solar cells. RSC Sustain. 2, 3036–3046. https://doi.org/10.1039/d4su00361f.
Khalifa, S.A., Spatari, S., Fafarman, A.T., Baxter, J.B., 2020. Environmental sustainability of mixed cation perovskite materials in photovoltaics manufacturing. ACS Sustain. Chem. Eng. 8, 16537–16548. https://doi.org/10.1021/acssuschemeng.0c05619.
Kralj, S., Lazarov, I., Woods-Robinson, R., Morales-Masis, M., 2025. Laboratory-scale reuse of Glass/ITO substrates for single junction perovskite solar cells. ACS Sustain. Chem. Eng. 13, 20787–20798. https://doi.org/10.1021/acssuschemeng.5c09075.
Larini, V., Ding, C., Wang, B., Pallotta, R., Faini, F., Pancini, L., et al., 2025. Circular management of perovskite solar cells using green solvents: from recycling and reuse of critical components to life cycle assessment. EES Solar 1, 378–390. https://doi.org/10.1039/D4EL00004H.
Lazard. *Lazard's Levelized Cost of Energy+*, 2025.
Leccisi, E., Fthenakis, V., 2024. Life-cycle human- and eco-toxicity assessment of emerging lead-based perovskite compared to conventional photovoltaic panels. MRS Bull. 49, 1240–1250. https://doi.org/10.1557/s43577-024-00812-8.
Lee, J.M., Kim, H.J., Jung, H.S., 2025. Life cycle assessment of lead recycling processes in perovskite solar cells. Chem. Commun. 61, 1850–1853. https://doi.org/10.1039/d4cc05121a.
Li, Q.X., Monticelli, C., Zanelli, A., 2022a. Life cycle assessment of organic solar cells and perovskite solar cells with graphene transparent electrodes. Renew. Energy 195, 906–917. https://doi.org/10.1016/j.renene.2022.06.075.
Li, Z., Li, B., Wu, X., Sheppard, S.A., Zhang, S.F., Gao, D.P., et al., 2022b. Organometallic-functionalized interfaces for highly efficient inverted perovskite solar cells. Science 376, 416–420. https://doi.org/10.1126/science.abm8566.
Lima, R., Bachmann, R.T., 2002. Pollutant emissions from modern incinerators. Int. J. Environ. Pollut. 18, 336–345. https://doi.org/10.1504/Ijep.2002.003731.
Liu, T.H., Chen, K., Hu, Q., Zhu, R., Gong, Q.H., 2016. Inverted perovskite solar cells: progresses and perspectives. Adv. Energy Mater. 6, 1600457. https://doi.org/10.1002/aenm.201600457.
Liu, Y.N., Duan, J.J., Zhang, J.K., Huang, S.M., Wei, O.Y., Bao, Q.Y., et al., 2020. High efficiency and stability of inverted perovskite solar cells using phenethyl ammonium iodide-modified interface of NiO and perovskite layers. ACS Appl. Mater. Inter. 12, 771–779. https://doi.org/10.1021/acsami.9b18217.
Llanos, M., Yekani, R., Demopoulos, G.P., Basu, N., 2020. Alternatives assessment of perovskite solar cell materials and their methods of fabrication. Renew. Sustain. Energy Rev. 133, 110207. https://doi.org/10.1016/j.rser.2020.110207.
Luu, L.Q., Cellura, M., Guarino, F., Longo, S., Rincione, R., 2026. Eco-design suggestions for innovative, lab-scaled perovskite solar cells. SSRN. https://doi.org/10.2139/ssrn.6255002.
Ma, X.T., Yao, X.J., Zhao, Y.Z., Zhu, G.Y., Zhong, H.L., 2025. Life cycle toxicity and reduction potential analysis of perovskite photovoltaic technology. J. Environ. Manag. 393, 127170. https://doi.org/10.1016/j.jenvman.2025.127170.
Maranghi, S., Parisi, M.L., Basosi, R., Sinicropi, A., 2019. Environmental profile of the manufacturing process of perovskite photovoltaics: harmonization of life cycle assessment studies. Energies 12, 3746. https://doi.org/10.3390/en12193746.
McCalmont, E., Ravilla, A., O'Hara, T., Carlson, B., Kellar, J., Celik, I., 2023. Life cycle cost assessment of material recovery from perovskite solar cells. MRS Adv. 8, 317–322. https://doi.org/10.1557/s43580-023-00542-0.
Mesquita, I., Andrade, L., Mendes, A., 2019. Temperature impact on perovskite solar cells under operation. ChemSusChem 12, 2186–2194. https://doi.org/10.1002/cssc.201802899.
NREL, 2026. Best research-cell efficiency chart. https://www.nrel.gov/pv/interactive-cell-efficiency.html accessed April 2026.
Okoroafor, T., Maalouf, A., Oez, S., Babu, V., Wilk, B., Resalati, S., 2022. Life cycle assessment of inkjet printed perovskite solar cells. J. Clean. Prod. 373, 133665. https://doi.org/10.1016/j.jclepro.2022.133665.
Osman, M., Qureshi, I., 2025. Review of photovoltaic and concentrated solar technologies including their performance, reliability, efficiency and storage. Results Eng. 25, 104424. https://doi.org/10.1016/j.rineng.2025.104424.
Pant, R., Castellani, V., Sala, S., Benini, L., De Laurentiis, V., Vidal Legaz, B., 2019. Suggestions for the Update of the Environmental Footprint Life Cycle Impact Assessment – Impacts due to Resource Use, Water Use, Land Use, and Particulate Matter. Publications Office of the European Union, Luxembourg.
Peel, M.C., Finlayson, B.L., McMahon, T.A., 2007. Updated world map of the Köppen-Geiger climate classification. Hydrol. Earth Syst. Sci. 11, 1633–1644. https://doi.org/10.5194/hess-11-1633-2007.
PlantMaps, 2024. Europe köppen climate classification map. https://www.plantmaps.com/koppen-climate-classification-map-europe.php accessed April 2024.
Principe, J., Duarte, V.C.M., Mendes, A., Andrade, L., 2023. Influence of the transparent conductive oxide type on the performance of inverted perovskite solar cells. ACS Appl. Energy Mater. 6, 12442–12451. https://doi.org/10.1021/acsaem.3c02292.
Principe, J., Duarte, V.C.M., Pereira, A.M.V.M., Mendes, A., Andrade, L., 2025. Highly efficient and cost-effective carbon paper electrode for inverted perovskite solar cells. Carbon 245. ARTN10.1016/j.carbon.2025.120830 120830.
Príncipe, J., Andrade, L., Mata, T.M., Martins, A.A., 2025. Comparative life cycle assessment of perovskite solar cell production: mesoporous n-i-p versus inverted p-i-n architectures. Adv. Energy Sustain. Res., 2400368 https://doi.org/10.1002/aesr.202400368.
Príncipe, J., Duarte, V.C.M., Andrade, L., 2022. Inverted perovskite solar cells: the emergence of a highly stable and efficient architecture. Energy Technol. Ger. 10, 2100952. https://doi.org/10.1002/ente.202100952.
Purkayastha, A., Minz, M., Sonkar, R.K., Mallajosyula, A.T., 2024. Efficiency enhancement and life cycle assessment of 2D/3D mixed-dimensional tin perovskite plasmonic solar cells. ACS Appl. Electr. Mater. 6, 737–747. https://doi.org/10.1021/acsaelm.3c01166.
Rao, H.K.R., Gemechu, E., Thakur, U., Shankar, K., Kumar, A., 2021. Life cycle assessment of high-performance monocrystalline titanium dioxide nanorod-based perovskite solar cells. Sol. Energy Mater. Sol. Cells 230, 111288. https://doi.org/10.1016/j.solmat.2021.111288.
Raugei, M., Sgouridis, S., Murphy, D., Fthenakis, V., Frischknecht, R., Breyer, C., et al., 2017. Energy Return on Energy Invested (ERoEI) for photovoltaic solar systems in regions of moderate insolation: a comprehensive response. Energy Policy 102, 377–384. https://doi.org/10.1016/j.enpol.2016.12.042.
Ravilla, A., Perini, C.A.R., Correa-Baena, J.P., Ho-Baillie, A.W.Y., Celik, I., 2024. Life cycle assessment of low-dimensional materials for perovskite photovoltaic cells. Energy Adv. 3, 800–811. https://doi.org/10.1039/d3ya00540b.
Rodriguez-Garcia, G., Aydin, E., De Wolf, S., Carlson, B., Kellar, J., Celik, I., 2021. Life cycle assessment of coated-glass recovery from perovskite solar cells. ACS Sustain. Chem. Eng. 9, 15239–15248. https://doi.org/10.1021/acssuschemeng.1c05029.
Rolf Frischknecht, P.S., Heath, Garvin, Raugei, Marco, 2020. Parikhit Sinha MdW-S *Methodology Guidelines on Life Cycle Assessment of Photovoltaic*; IEA-PVPS T12-18: 2020. International Energy Agency.
Rossi, F., Rotondi, L., Stefanelli, M., Sinicropi, A., Vesce, L., Parisi, M.L., 2024. Comparative life cycle assessment of different fabrication processes for perovskite solar mini-modules. Epj Photovolt. 15, 20. https://doi.org/10.1051/epjpv/2024014.
Said, A.A., Xie, J., Zhang, Q.C., 2019. Recent progress in organic electron transport materials in inverted perovskite solar cells. Small 15, 1900854. https://doi.org/10.1002/smll.201900854.
Sarialtin, H., Geyer, R., Zafer, C., 2020. Life cycle assessment of hole transport free planar-mesoscopic perovskite solar cells. J. Renew. Sustain. Energy 12, 023502. https://doi.org/10.1063/1.5129784.
Statistical, 2023. Cumulative installed solar PV capacity worldwide from 2000 to 2022. https://www.statista.com/statistics/280220/global-cumulative-installed-solar-pv-capacity/ accessed November 2023.
Steinmüller Babcock Environment. Flue gas cleaning. https://www.hzi-steinmueller.com/wp-content/uploads/downloads/broschure-flue-gas-cleaning-en.pdf accessed September 2025.
Tian, X.Y., Stranks, S.D., You, F.Q., 2021. Life cycle assessment of recycling strategies for perovskite photovoltaic modules. Nat. Sustain. 4, 821–829. https://doi.org/10.1038/s41893-021-00737-z.
Trinomics BV *Energy Costs, Taxes and the Impact of Government Interventions on Investments - Final Report*; 9276231242, 2020. Publications Office of the European Union.
Tsang, M.P., Sonnemann, G.W., Bassani, D.M., 2016. A comparative human health, ecotoxicity, and product environmental assessment on the production of organic and silicon solar cells. Prog. Photovoltaic. 24, 645–655. https://doi.org/10.1002/pip.2704.
United Nations Framework Convention on Climate Change, 2015. What is the Paris agreement? In: https://unfccc.int/process-and-meetings/the-paris-agreement accessed November 2023.
U.S. Energy Information Administration, 2025. Levelized Costs of New Generation Resources in Annual Energy Outlook 2025.
Valderrama, Benítez CA., Molina Pérez, F.J., Montoya Arango, J.F., Rodríguez, D.C., Villa, A.L., Alberola-Borràs, J.-A., 2025. Evaluation of environmental impacts of a perovskite solar cell with a p-i-n meso-superstructured architecture through life cycle assessment. Sustain. Energy Fuels 9, 2753–2768. https://doi.org/10.1039/D4SE01571A.
Vidal, R., Alberola-Borràs, J.A., Sánchez-Pantoja, N., Mora-Seró, I., 2021. Comparison of perovskite solar cells with other photovoltaics technologies from the point of view of life cycle assessment. Adv. Energy Sustain. Res. 2, 2000088. https://doi.org/10.1002/aesr.202000088.
Wang, Q., Xie, Y., Soltani-Kordshuli, F., Eslamian, M., 2016. Progress in emerging solution-processed thin film solar cells - part I: polymer solar cells. Renew. Sustain. Energy Rev. 56, 347–361. https://doi.org/10.1016/j.rser.2015.11.063.
Weyand, S., Kawajiri, K., Mortan, C., Zeller, V., Schebek, L., 2023. Are perovskite solar cells an environmentally sustainable emerging energy technology? Upscaling from lab to fab in life cycle assessment. ACS Sustain. Chem. Eng. 11, 14010–14019. https://doi.org/10.1021/acssuschemeng.3c03019.

Wu, P.F., Wang, S.R., Li, X.G., Zhang, F., 2022. Beyond efficiency fever: preventing lead leakage for perovskite solar cells. Matter-Us 5, 1137–1161. https://doi.org/10.1016/j.matt.2022.02.012.

Xu, L., Chen, X.F., Jin, J.J., Liu, W., Dong, B., Bai, X., et al., 2019. Inverted perovskite solar cells employing doped NiO hole transport layers: a review. Nano Energy 63, 103860. https://doi.org/10.1016/j.nanoen.2019.103860.

Yue, D.J., You, F.Q., Darling, S.B., 2014. Domestic and overseas manufacturing scenarios of silicon-based photovoltaics: life cycle energy and environmental comparative analysis. Sol. Energy 105, 669–678. https://doi.org/10.1016/j.solener.2014.04.008.

Zhang, Y., Bakshi, B.R., Demessie, E.S., 2008. Life cycle assessment of an ionic liquid versus molecular solvents and their applications. Environ. Sci. Technol. 42, 1724–1730. https://doi.org/10.1021/es0713983.

Zhao, G.L., Hughes, D., Beynon, D., Wei, Z.F., Watson, T., Tsoi, W.C., et al., 2024. Perovskite photovoltaics for aerospace applications - life cycle assessment and cost analysis. Sol. Energy 274, 112602. https://doi.org/10.1016/j.solener.2024.112602.